Los Alamos
NATIONAL LABORATORY
EST. 1943

LA-UR-21-26108
Approved for public release; distribution is unlimited.

Title: From the LHC and RHIC to the EIC: Probing QCD

Author(s): Khatiwada, Ajeeta

Intended for: Seminar

Issued: 2021-06-29

Disclaimer:
Los Alamos National Laboratory, an affirmative action/equal opportunity employer, is operated by Triad National Security, LLC for the National Nuclear Security Administration of U.S. Department of Energy under contract 89233218CNA000001. By approving this article, the publisher recognizes that the U.S. Government retains nonexclusive, royalty-free license to publish or reproduce the published form of this contribution, or to allow others to do so, for U.S. Government purposes. Los Alamos National Laboratory requests that the publisher identify this article as work performed under the auspices of the U.S. Department of Energy. Los Alamos National Laboratory strongly supports academic freedom and a researcher's right to publish; as an institution, however, the Laboratory does not endorse the viewpoint of a publication or guarantee its technical correctness.

From the LHC and RHIC to the EIC: Probing QCD

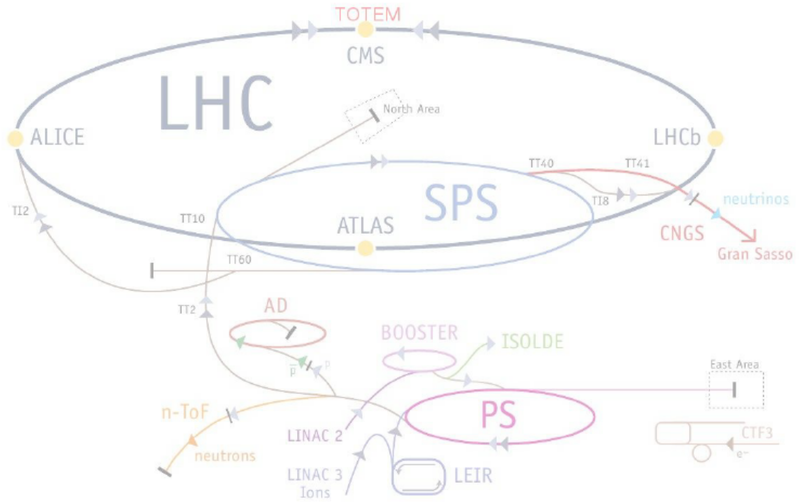

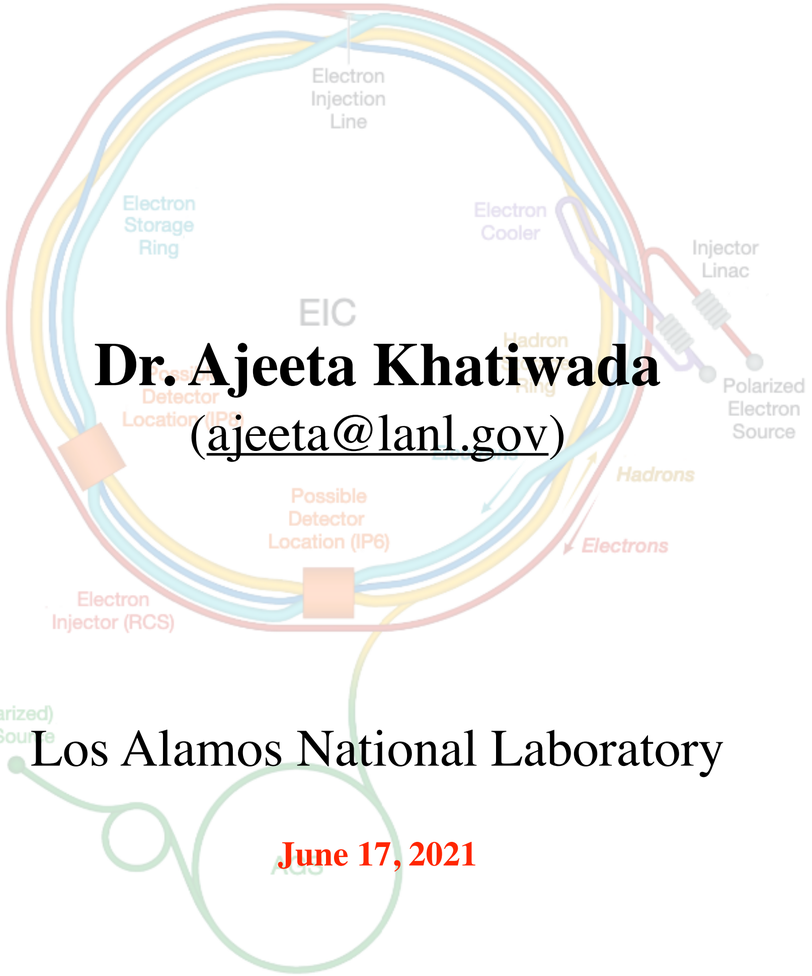

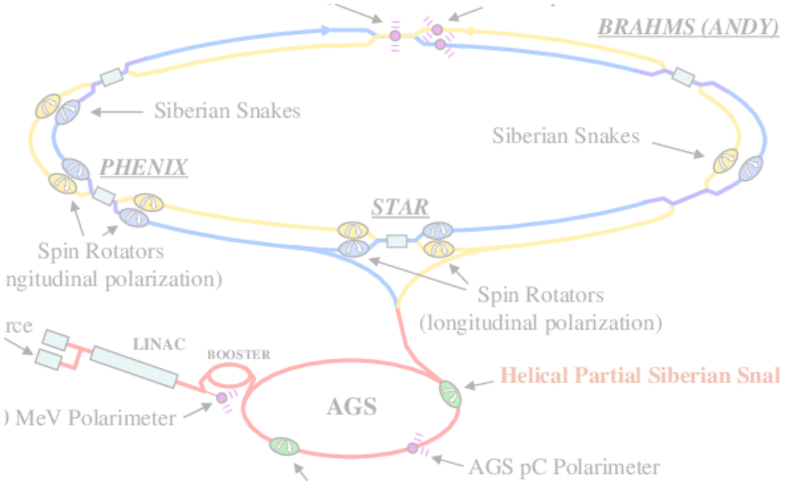

Dr. Ajeeta Khatiwada
(ajeeta@lanl.gov)

Los Alamos National Laboratory

June 17, 2021

Professional summary

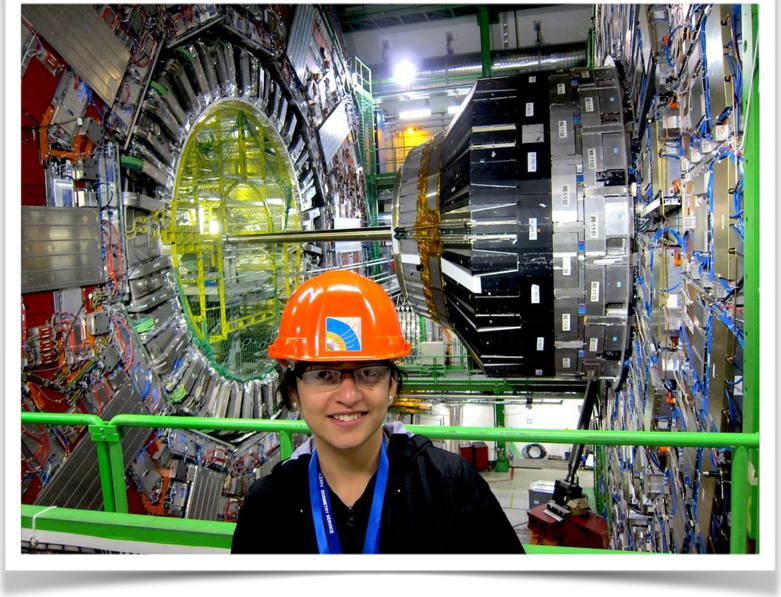

- PhD in Experimental High Energy Physics — Florida State University, Tallahassee, Florida (2016)
  - Photon+jet cross section analysis using data from the CMS experiment at LHC, CERN.
- Postdoc — Purdue University, stationed at Fermilab (2016 — 2018)
  - Top quark pair spin correlation and polarization using data from the CMS experiment at LHC, CERN.
- Postdoc — Los Alamos National Lab (2018 — present)
  - Decay of heavy flavor hadrons to single muons using data from PHENIX detector at RHIC, BNL.
  - X-ray radiography with a team of LANL scientists in physics and theory division.

Outline

- Understanding gluon PDFs using photon+jet cross section measurement from the CMS pp data
- Heavy flavor “tagging”/classification using Machine Learning tools at PHENIX
- Unfolding development for top quark pair spin correlation and polarization at the CMS
- Other contributions to the CMS and PHENIX
- My interests in the EIC physics

Outline

- Understanding gluon PDFs using photon+jet cross section measurement from the CMS pp data
- Heavy flavor “tagging”/classification using Machine Learning tools at PHENIX
- Unfolding development for top quark pair spin correlation and polarization at the CMS
- Other contributions to the CMS and PHENIX
- My interests in the EIC physics

Inclusive isolated-photon+jet in pp collisions at CMS

Dominant

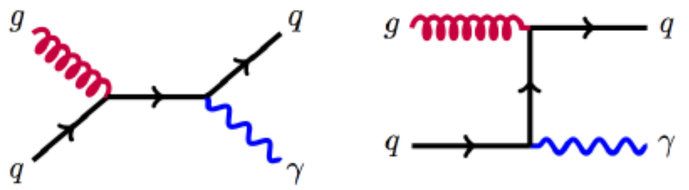

quark-gluon Compton scattering

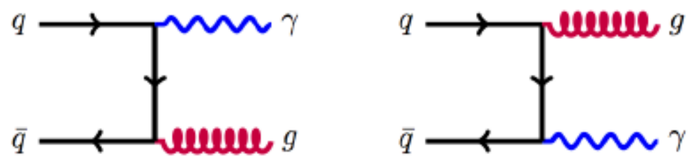

$q\bar{q}$ annihilation

Suppressed with isolation cuts

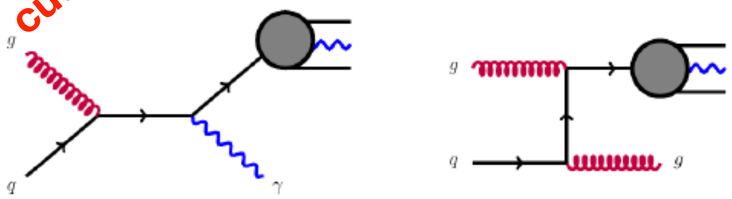

fragmentation

➡ Photon+jet measurements are excellent probes of QCD and gluon distribution functions.

Inclusive isolated-photon+jet in pp collisions at CMS

Dominant

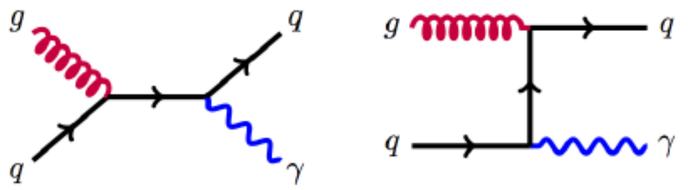

quark-gluon Compton scattering

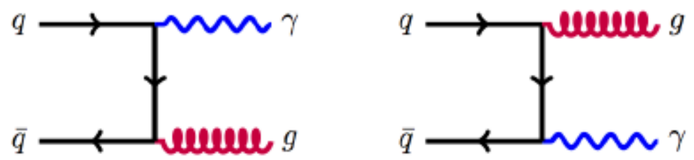

$q\bar{q}$ annihilation

Suppressed with isolation cuts

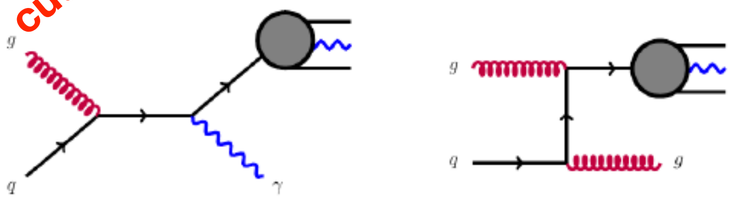

fragmentation

$$\frac{d^3\sigma}{dp_\gamma^3}(AB \to \gamma X) = \frac{1}{E_\gamma}\sum_{abcd}\int dx_a dx_b dz_c$$

$$f_{a/A}(x_a, Q^2) f_{b/B}(x_b, Q^2) D_{C/c}(z_c, Q^2)$$

$$\frac{\hat{s}}{z_c^2\pi}\frac{d\sigma}{d\hat{t}}(ab \to cd) \times \delta(\hat{s} + \hat{t} + \hat{u})$$

- Photon+jet measurements are excellent probes of QCD and gluon distribution functions.
- Total cross section at the hadron collider consists of perturbatively calculable parton level cross section and non perturbative hadronic matrix elements.

Inclusive isolated-photon+jet in pp collisions at CMS

Dominant

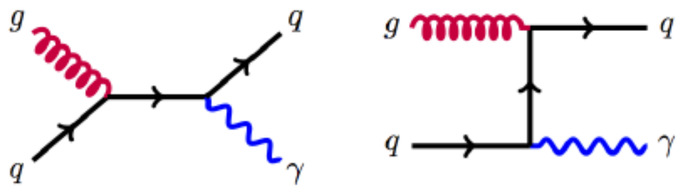

quark-gluon Compton scattering

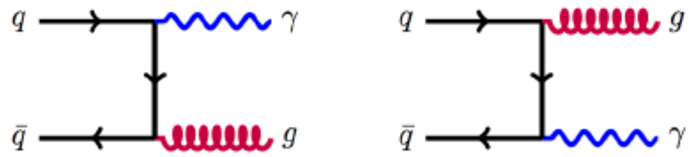

$q\bar{q}$ annihilation

Suppressed with isolation cuts

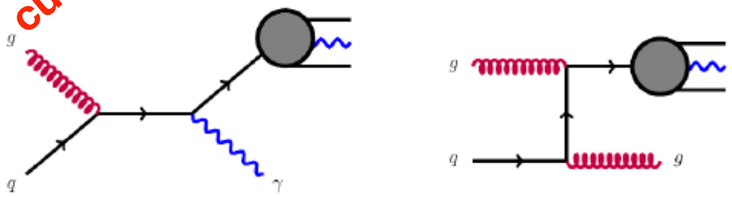

fragmentation

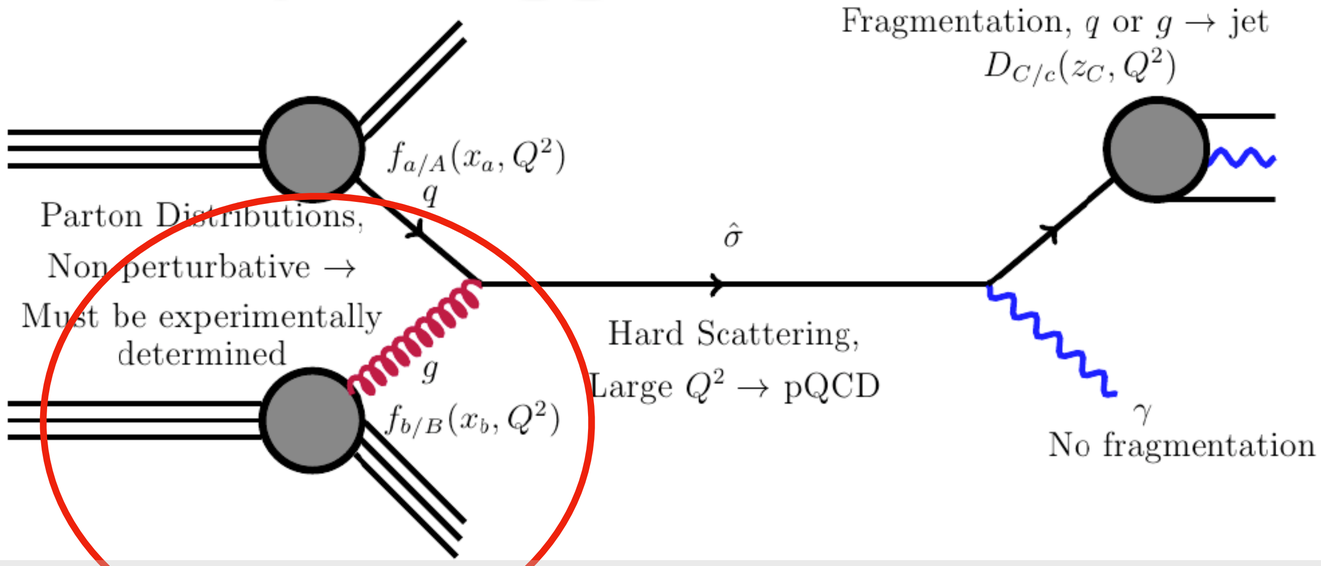

- Photon+jet measurements are excellent probes of QCD and gluon distribution functions.
- Total cross section at the hadron collider consists of perturbatively calculable parton level cross section and non perturbative hadronic matrix elements.

Inclusive isolated-photon+jet in pp collisions at CMS

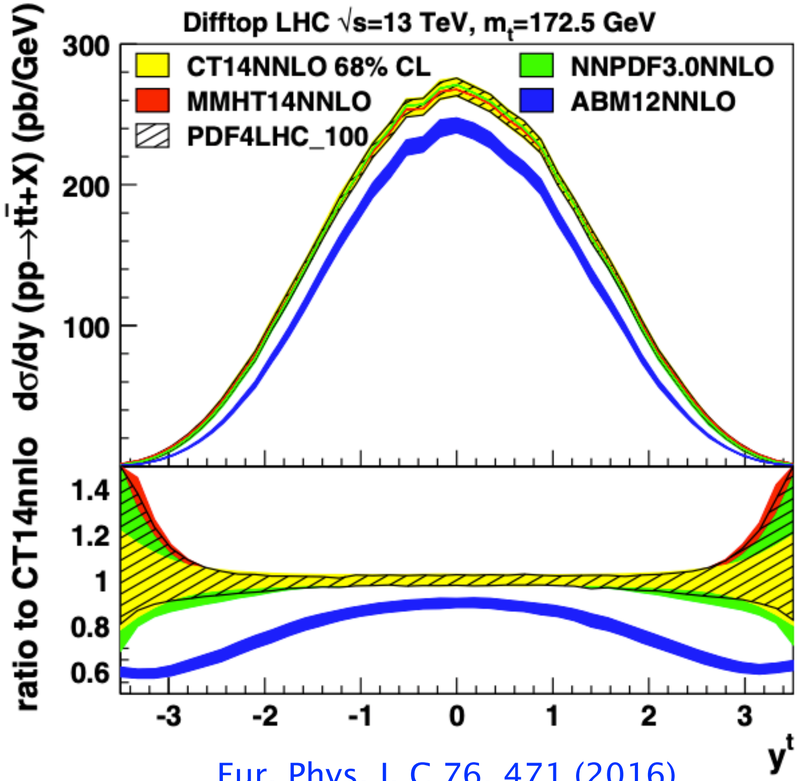

Eur. Phys. J. C 76, 471 (2016)

Top-quark pair production cross sections at approximate NNLO as a function of the top-quark rapidity using different PDFs at NNLO with the respective PDF uncertainty

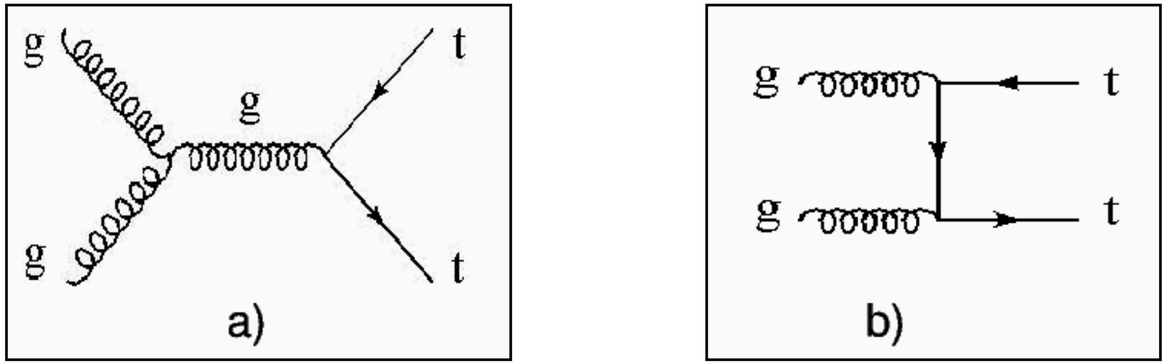

Top pair production through gluon fusion @ LO

- Photon+jet measurements are excellent probes of QCD and gluon distribution functions.
- Total cross section at the hadron collider consists of perturbatively calculable parton level cross section and non perturbative hadronic matrix elements.
- Improved understanding of PDFs is key to reducing theoretical uncertainties in other measurements such as Higgs boson production, top quark pair production, and new physics searches.

Photon & jet reconstruction and Id with the CMS

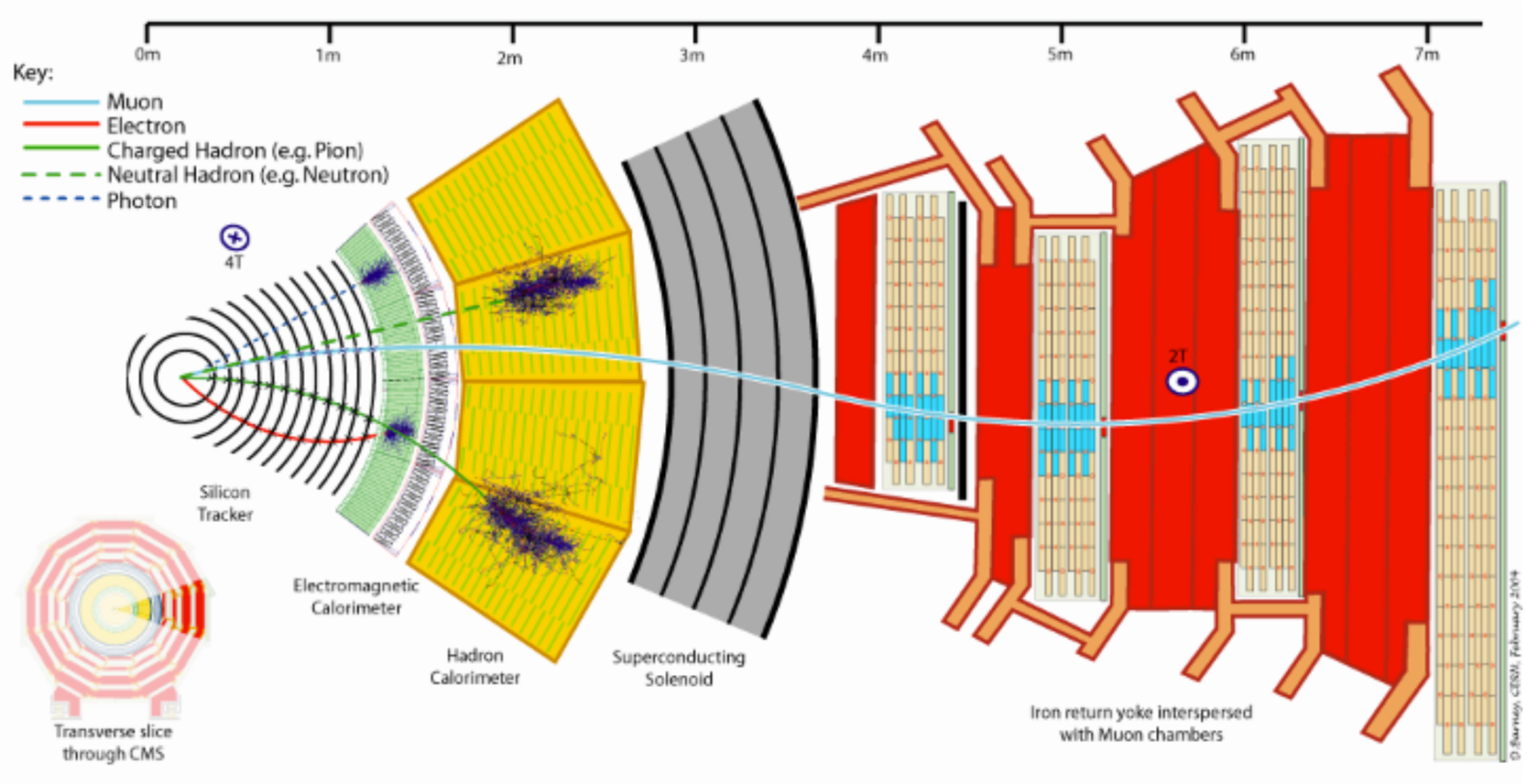

Photon & jet reconstruction and Id with the CMS

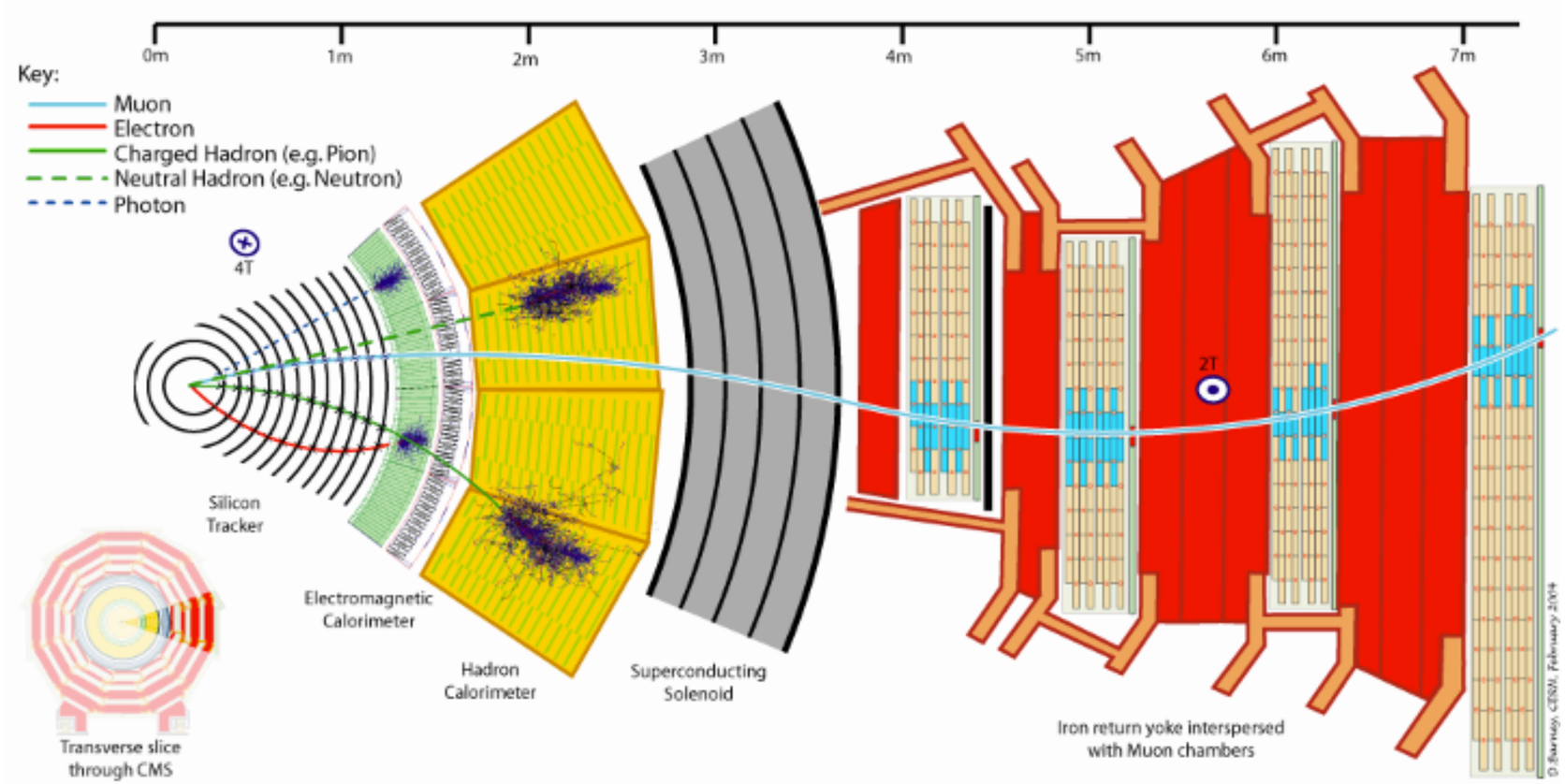

Photons are reconstructed using ECAL clusters

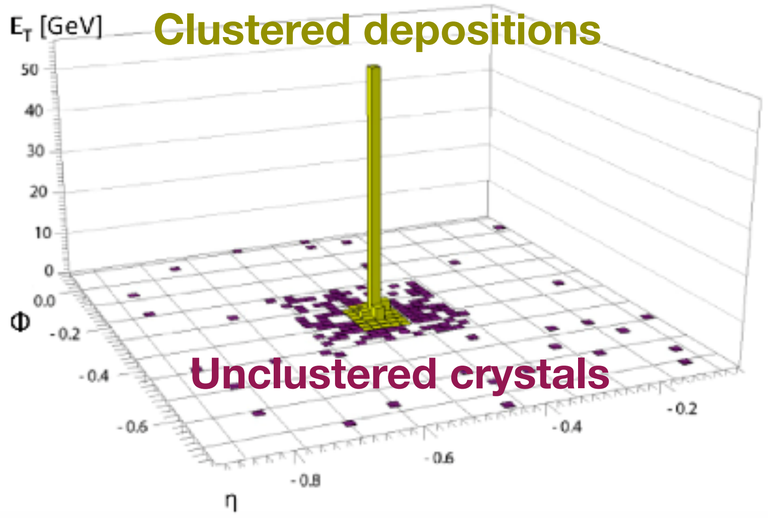

Photon & jet reconstruction and Id with the CMS

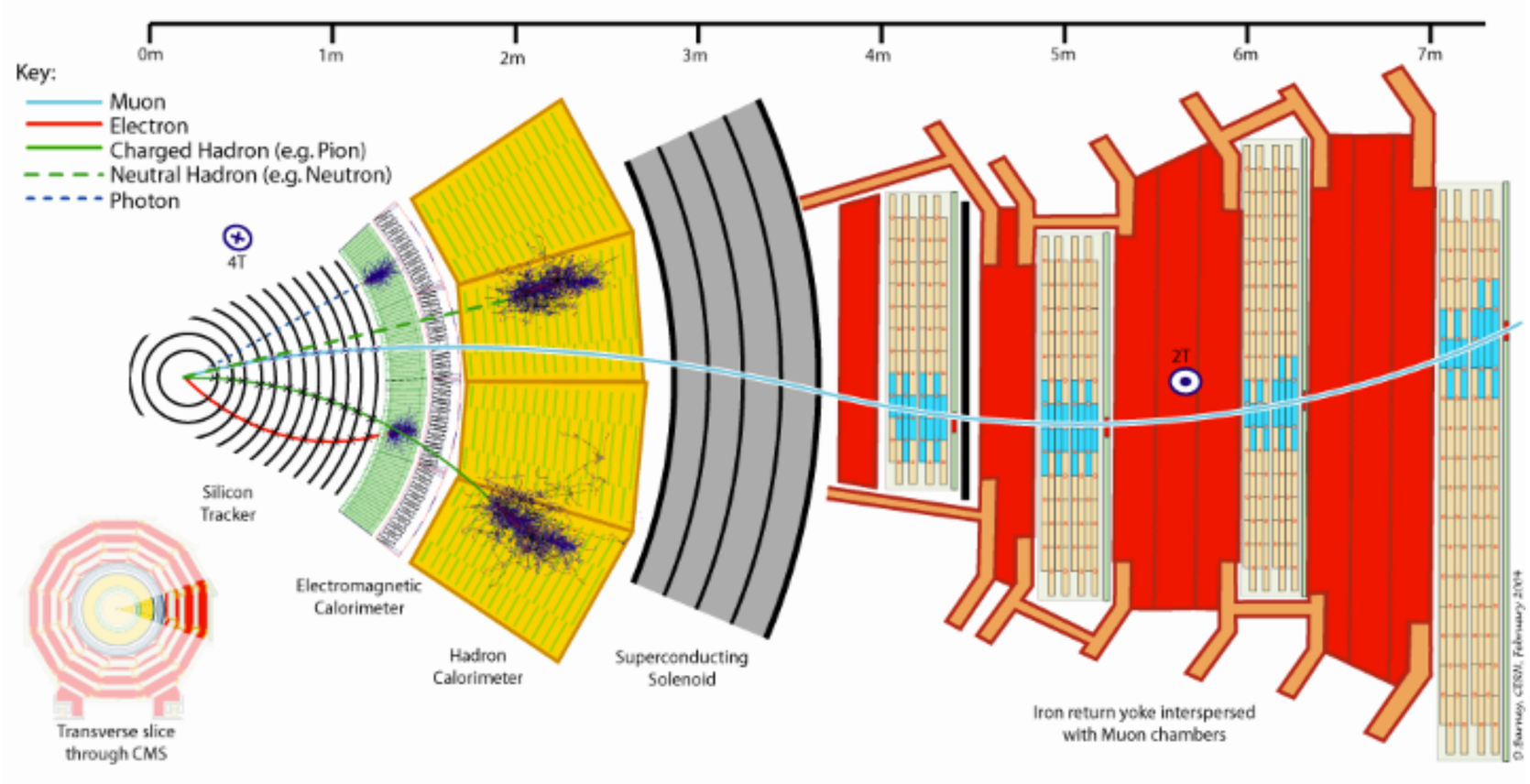

Photons are reconstructed using ECAL clusters

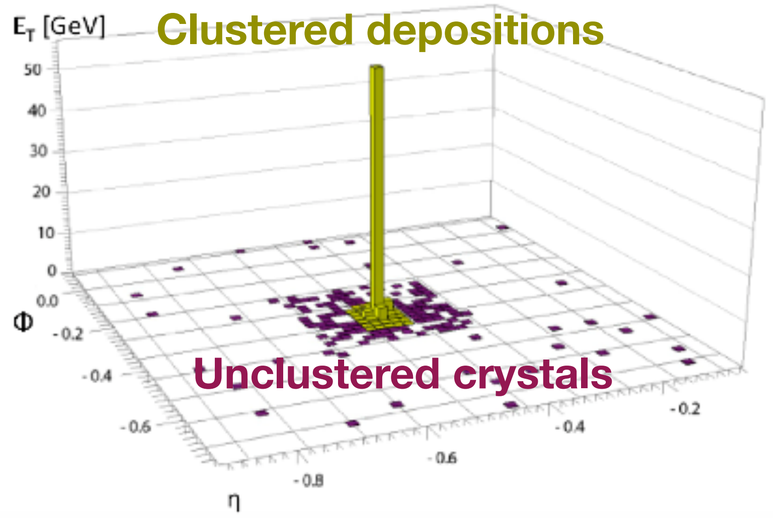

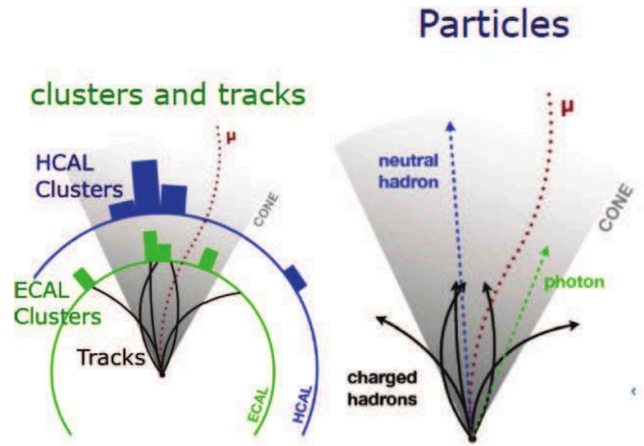

Particle Flow Jets clustered using anti-k_T algorithm with $\Delta R = 0.5$

Using Machine Learning in high background environment

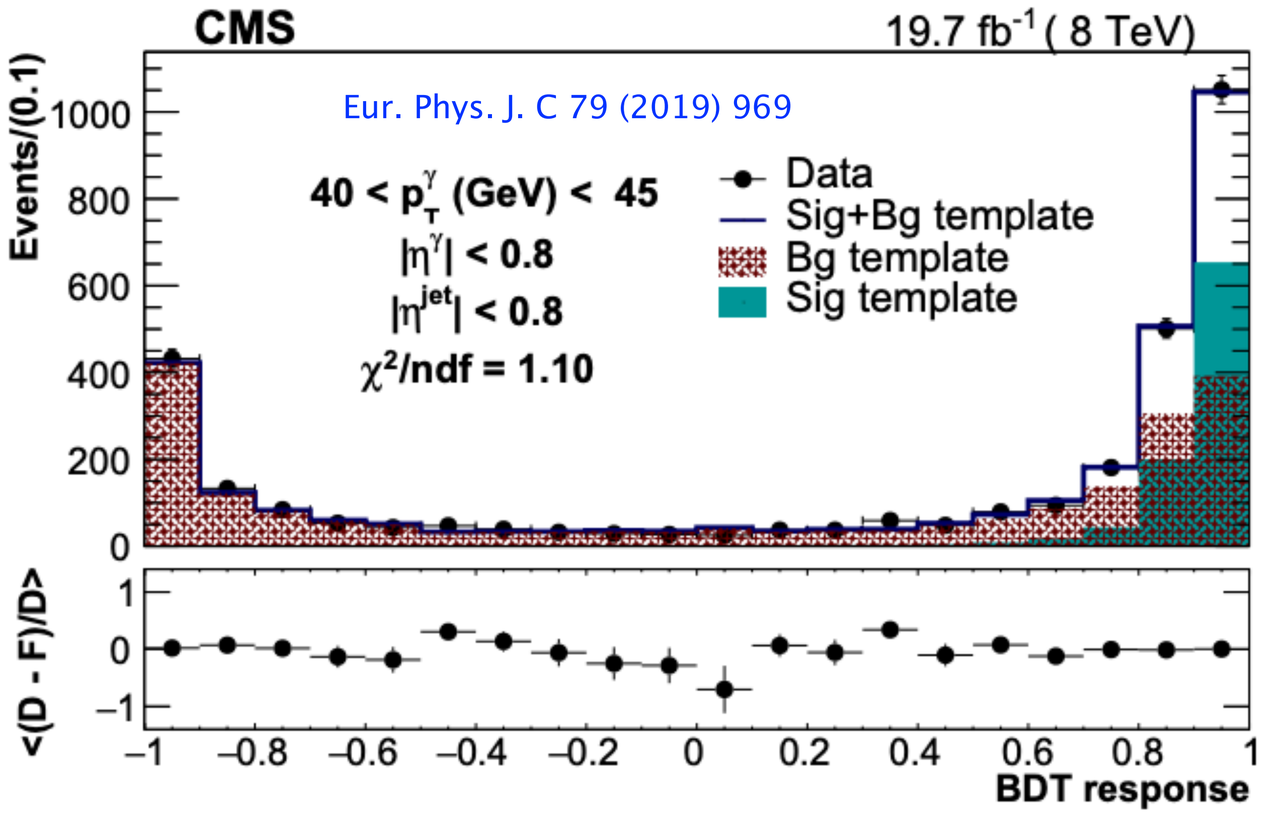

- ML output fit to get the signal purity from QCD multijet background.
- At the time when the analysis was started this was a novel technique.

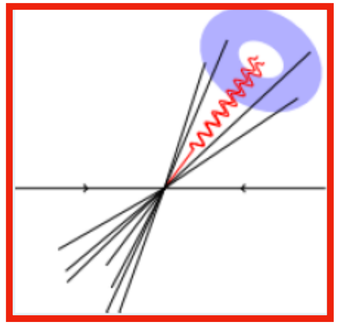

Using Machine Learning in high background environment

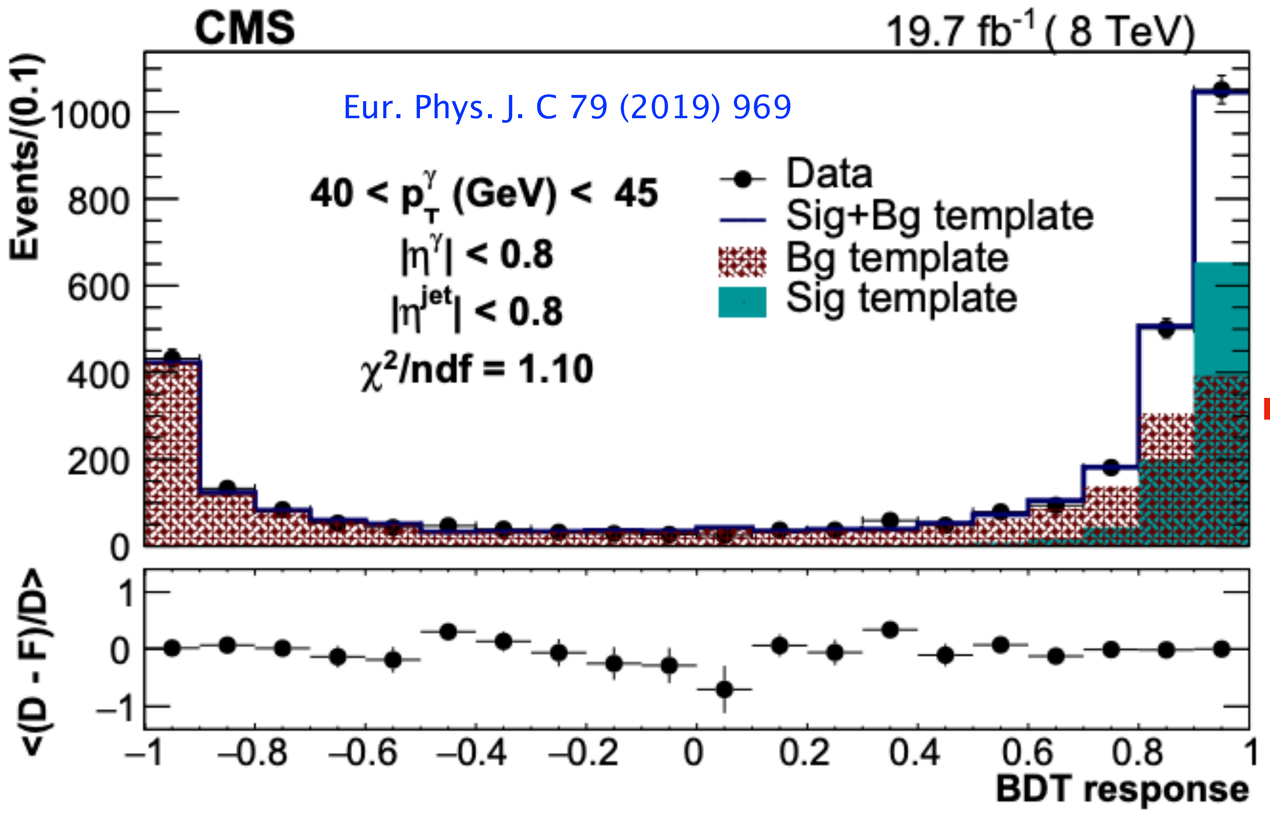

Scan over data sideband phase space in photon isolation to determine a region in data that describes the multijet background in the signal region.

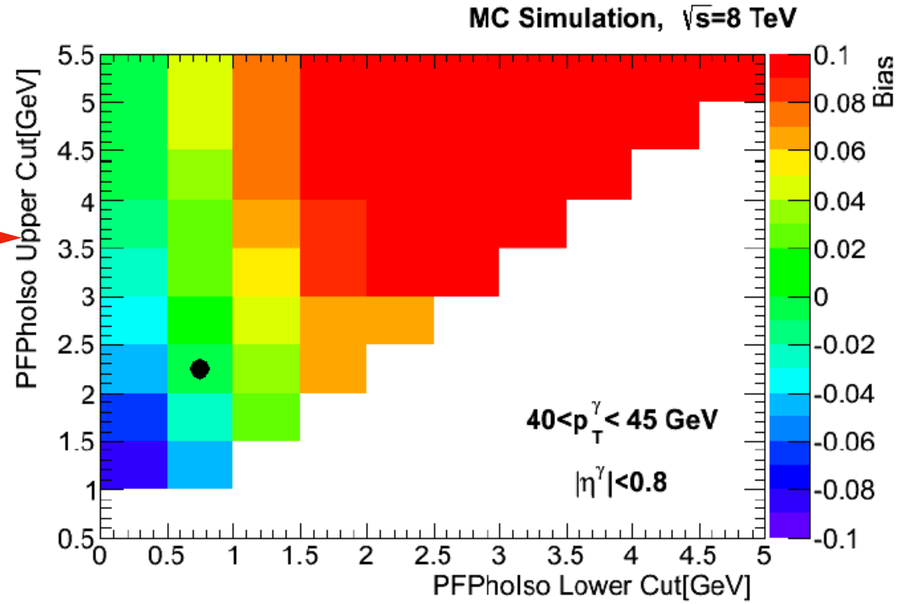

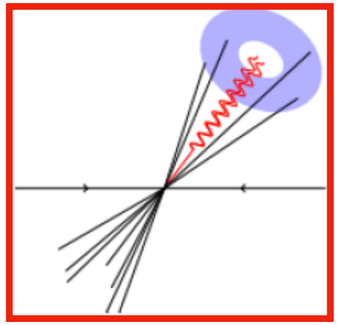

- ML output fit to get the signal purity from QCD multijet background.
- At the time when the analysis was started this was a novel technique.

Triple differential cross section measurement

➡ Some examples of the measurement in different kinematic regions of photon and jet

Eur. Phys. J. C 79 (2019) 969

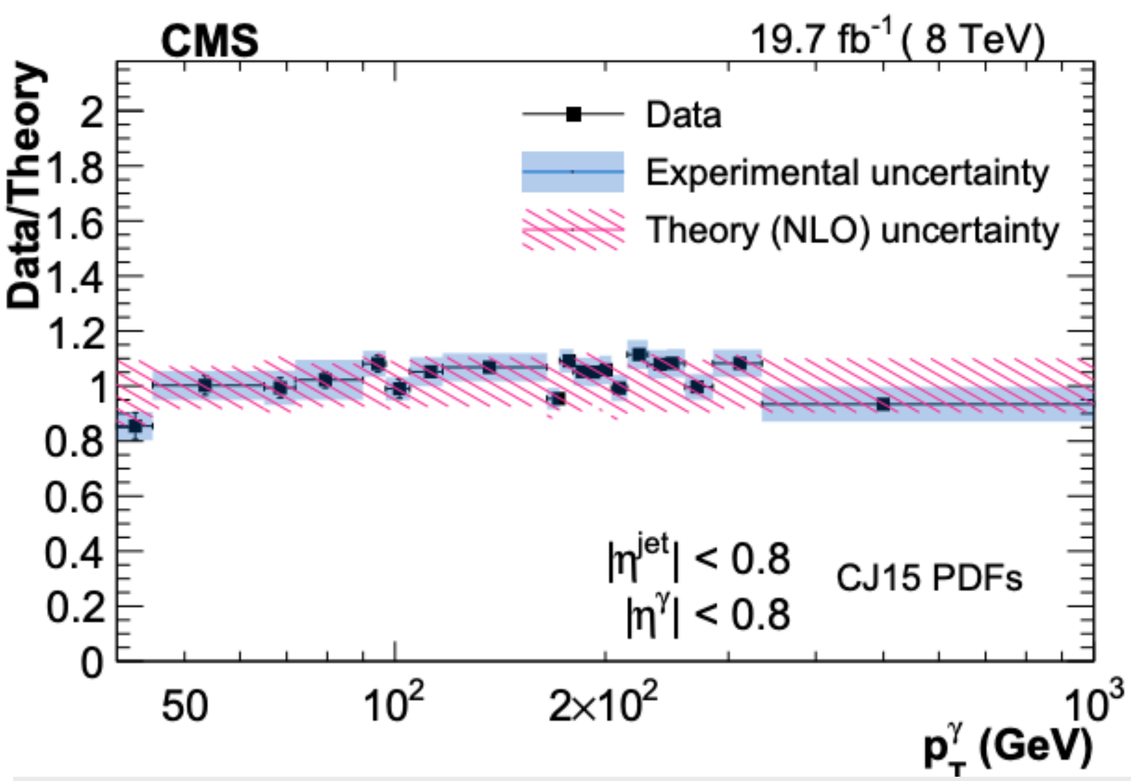

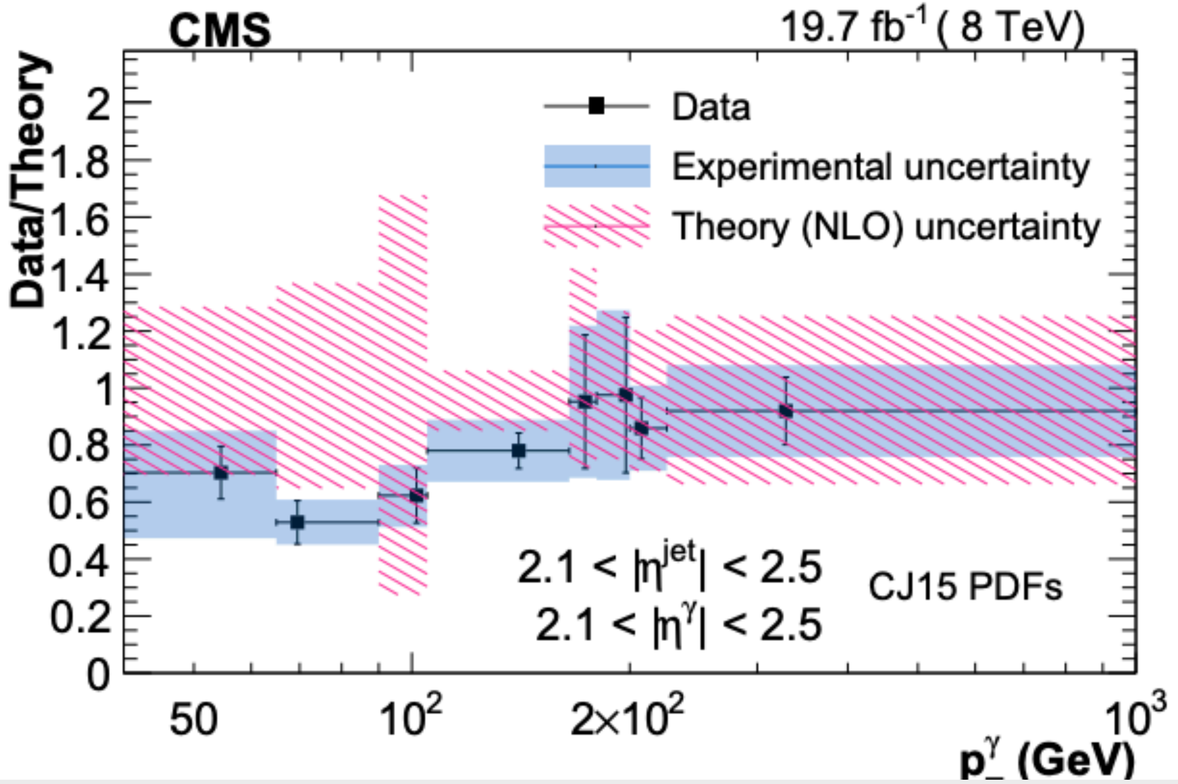

➡ Measurement in total 224 bins in photon p_T, photon pseudorapidity and jet pseudorapidity combinations.

➡ In agreement with NLO QCD predictions, and in many bins more precise than the theoretical calculations given the PDF & scale uncertainties.

Probing the gluon PDF with direct photons @ LHC

- Photon+jet measurements were discontinued in global PDF fits until recently.

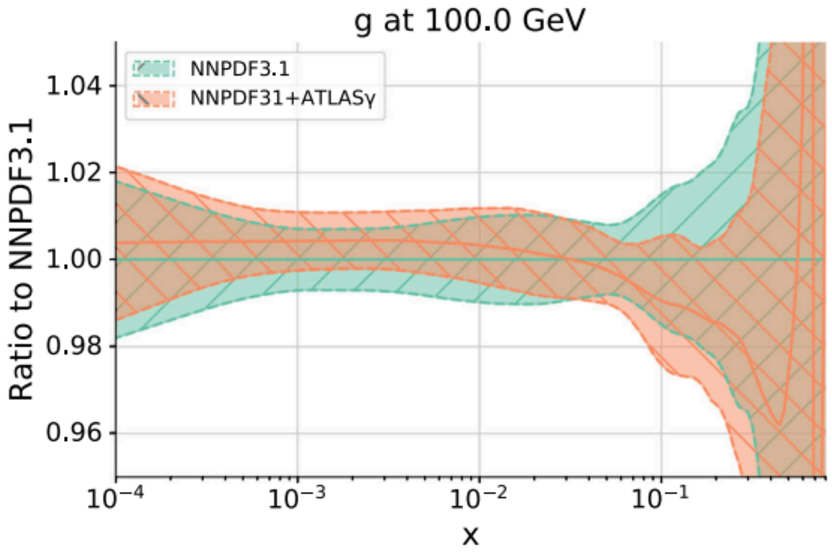

- Inclusion of ATLAS 8 TeV isolated photon measurement shows more constrained gluon PDF over large range of parton momentum fraction, x, for NNPDF3.1

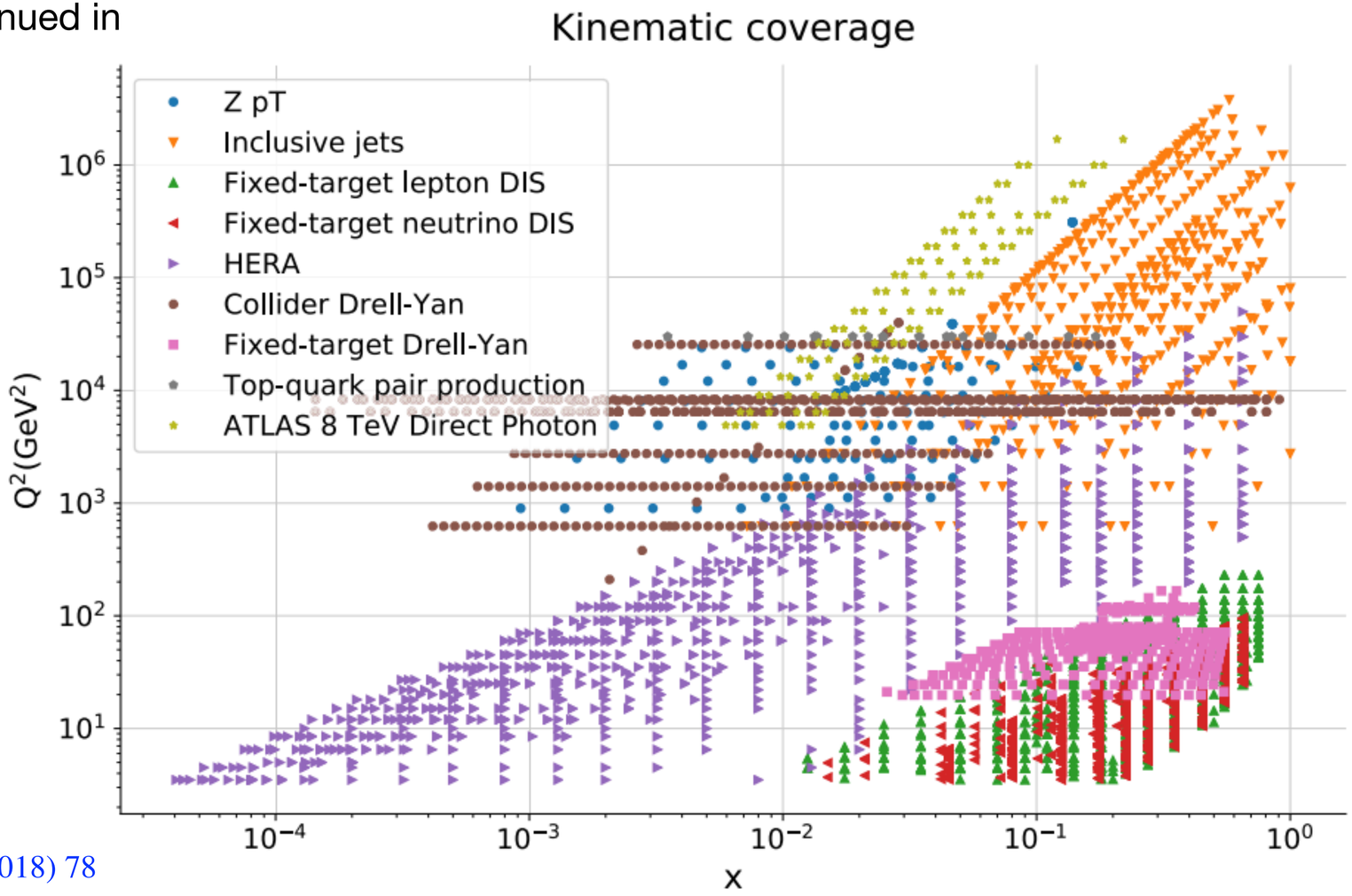

Eur. Phys. J. C (2018) 78

Impact of my work

- CMS measurement in an isolated-photon+jet triple differential cross section measurement w.r.t photon p_T, photon pseudorapidity and jet pseudorapidity:

$$x = \frac{p_T^{\gamma}}{\sqrt{s}}(e^{\pm\eta^{\gamma}} + e^{\pm\eta^{jet}})$$

- Combination of the photon and jet eta can probe a wide range of x.

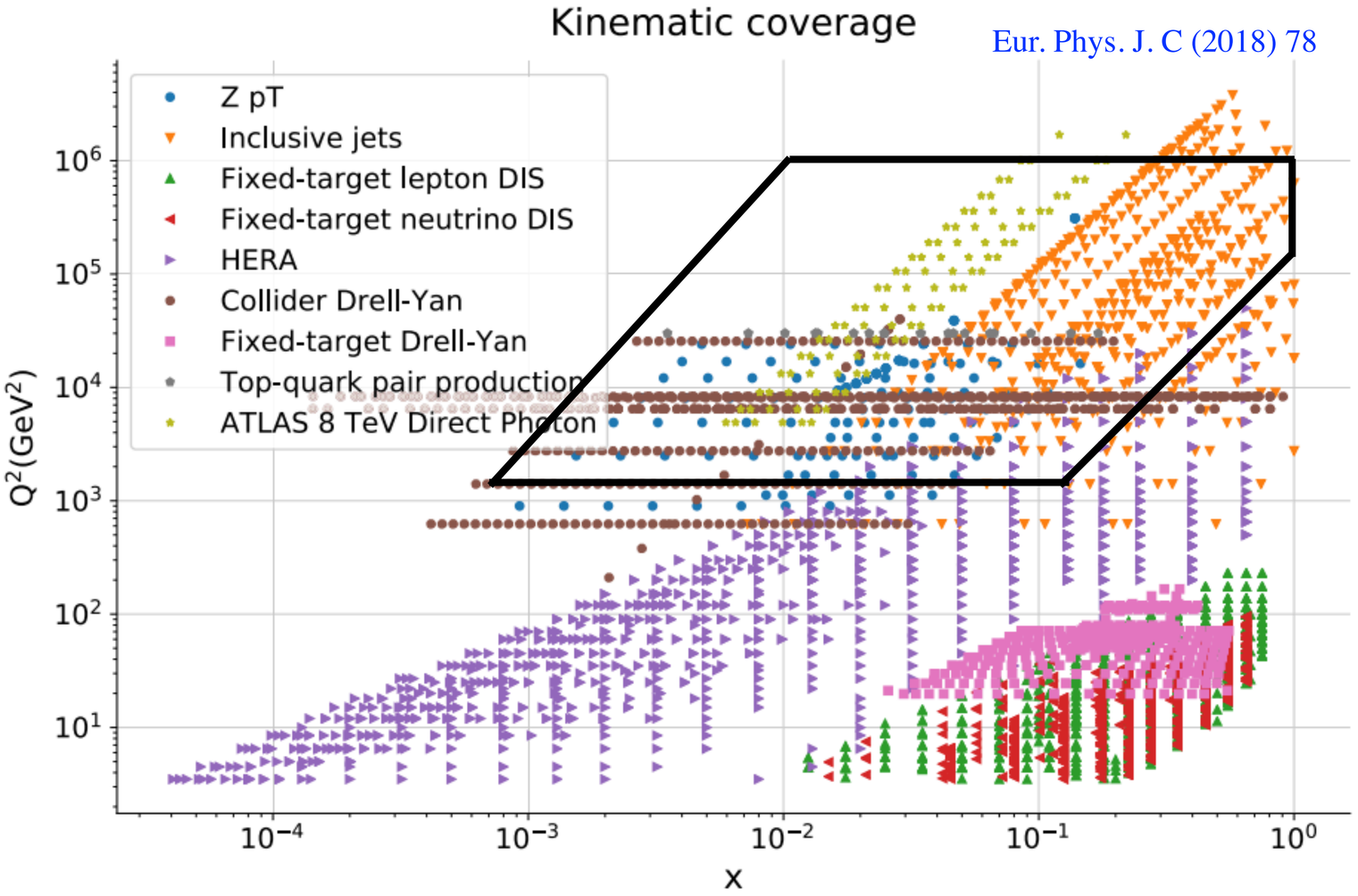

Eur. Phys. J. C (2018) 78

Outline

- Understanding gluon PDFs using photon+jet cross section measurement from the CMS pp data
- Heavy flavor “tagging”/classification using Machine Learning tools at PHENIX
- Unfolding development for top quark pair spin correlation and polarization at the CMS
- Other contributions to the CMS and PHENIX
- My interests in the EIC physics

Heavy flavors as a probe of cold and hot nuclear matter

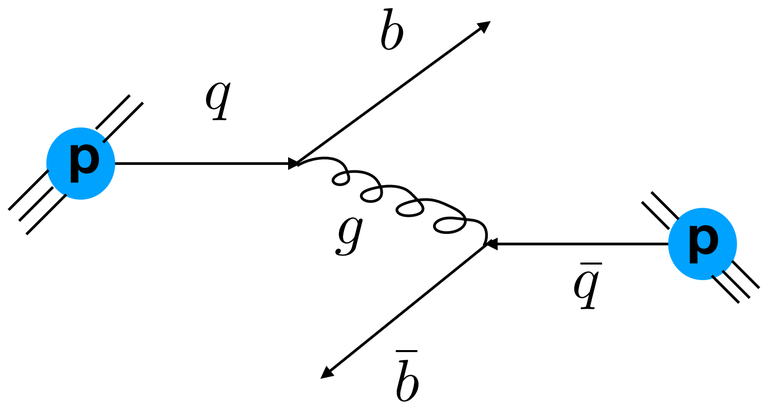

Heavy flavor production at LO

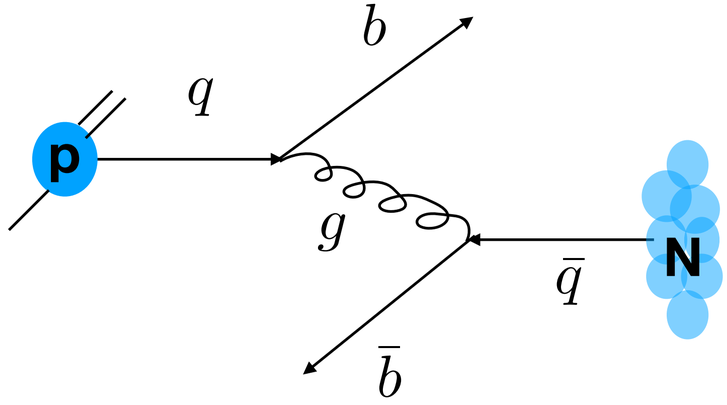

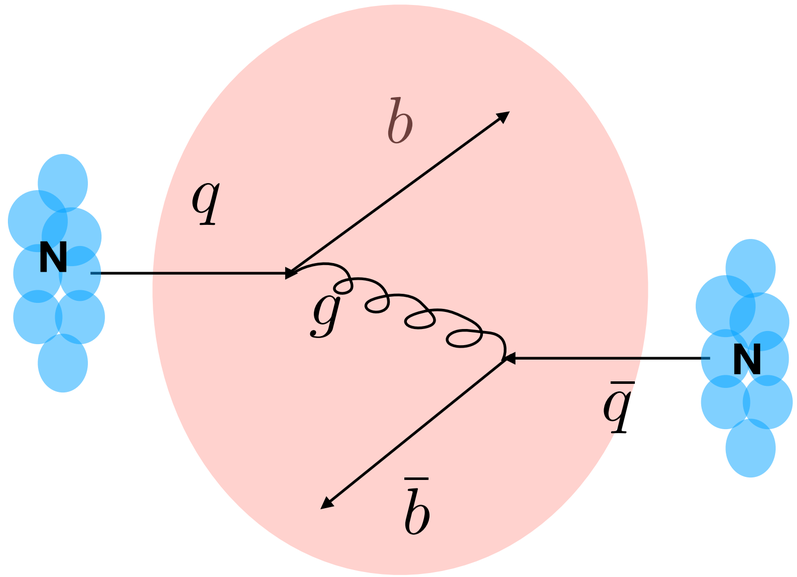

$$m_b > m_c > \Lambda_{QCD}, T_c$$

4.2 GeV 1.3 GeV 0.2 GeV

➡ Low p_T (collisional energy loss dominant): partially thermalize in Quark Gluon Plasma (QGP) medium?

➡ High p_T (radiative energy loss dominant): mass dependent energy loss in QGP?

Heavy flavors as a probe of cold and hot nuclear matter

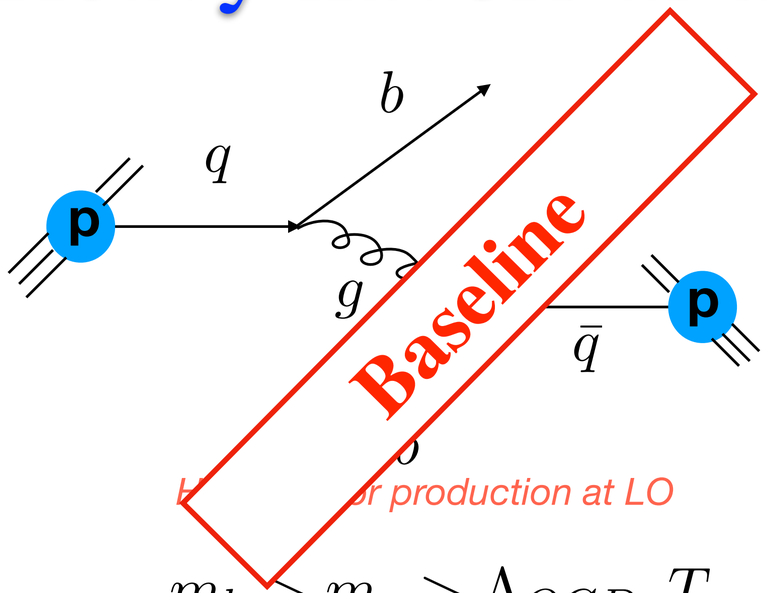

$$m_b > m_c > \Lambda_{QCD}, T_c$$

4.2 GeV 1.3 GeV 0.2 GeV

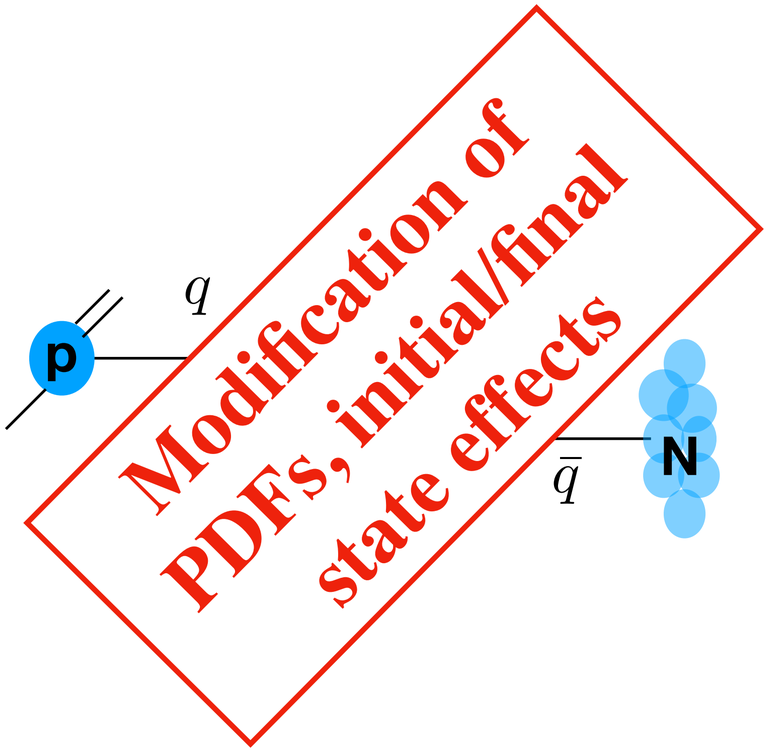

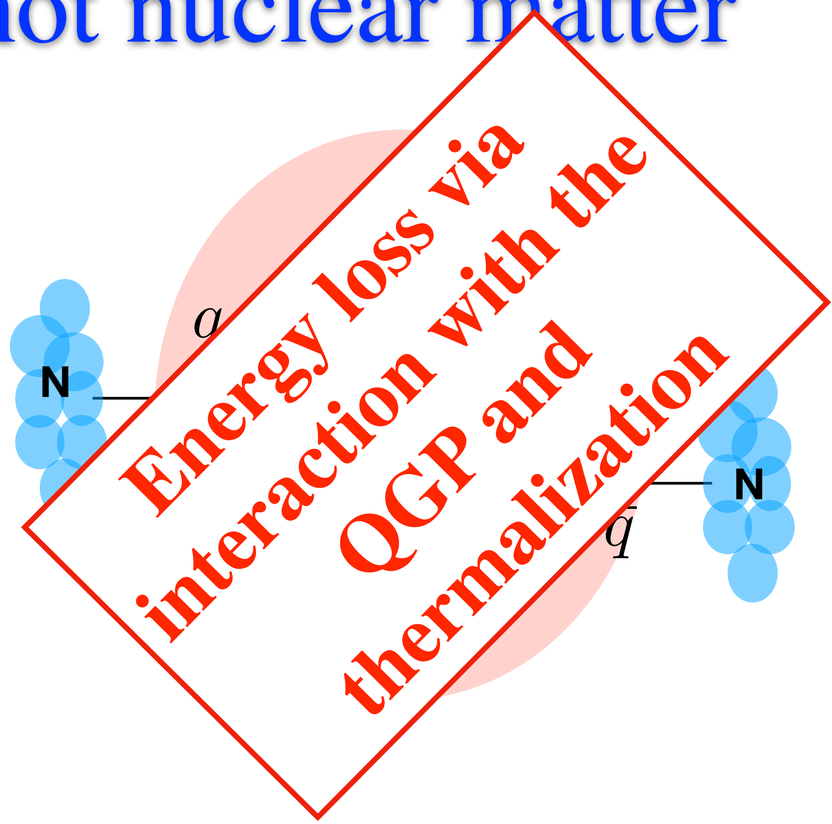

➡ Low p_T (collisional energy loss dominant): partially thermalize in Quark Gluon Plasma (QGP) medium?

➡ High p_T (radiative energy loss dominant): mass dependent energy loss in QGP?

Previous efforts to study flavor dependent energy loss in mid-rapidity

- At low p_T:
  - Higher $c \rightarrow e$ suppression than $b \rightarrow e$.
  - Consistent with the expected mass dependence: $\Delta E_g > \Delta E_{u,d,s} > \Delta E_c > \Delta E_b$
- At high p_T:
  - Poor systematic precision & narrow coverage in p_T particularly due to pp baseline.
- Single muons from separated D/B hadrons have not been studied at forward rapidities. PHENIX has a unique ability to probe QGP at low momentum and forward rapidity bins.

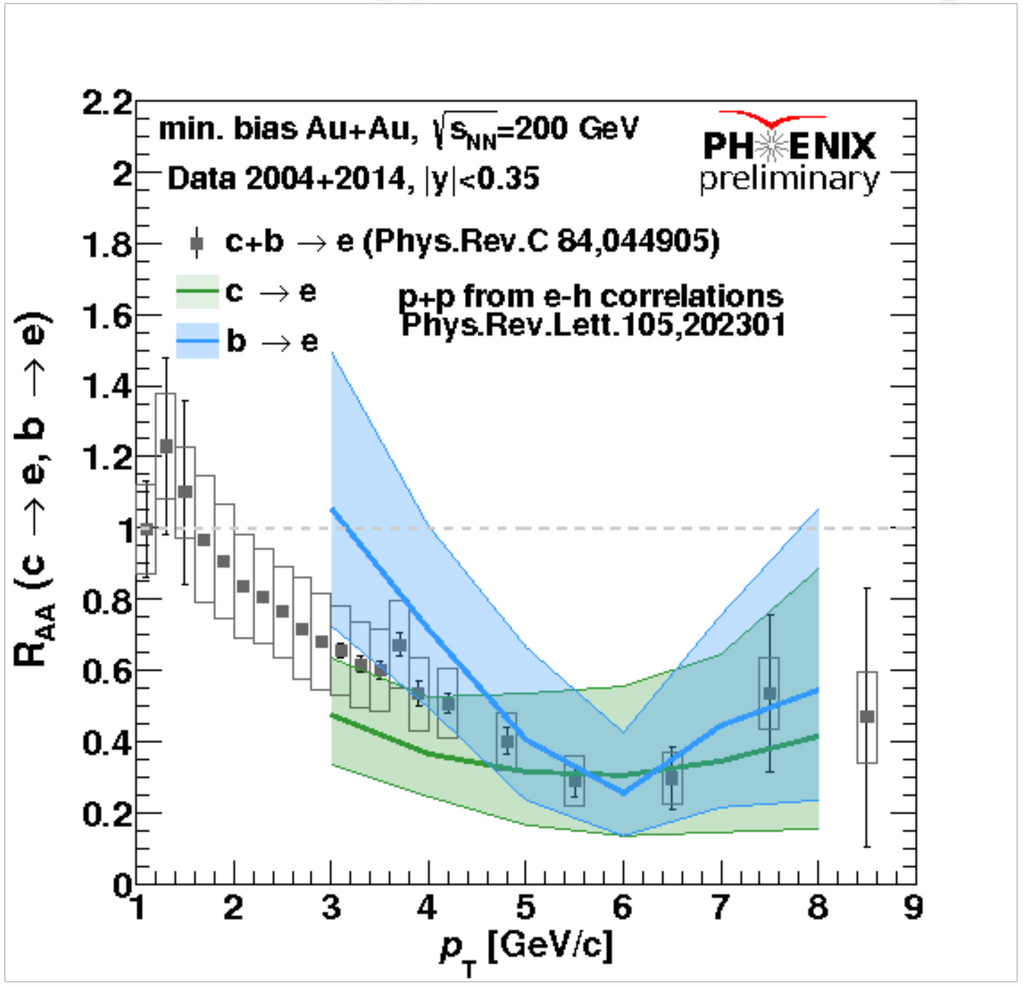

$$R_{AA} = \frac{1}{< N_{coll} >} \frac{(dN/dy)^{AA}}{(dN/dy)^{pp}}$$

Studying semi-leptonic decay of heavy flavors with the muon arms

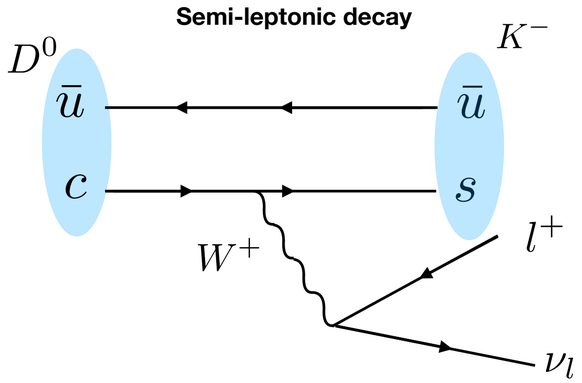

Muons from semi-leptonic decay of HF measured in muon arm in the forward/backward region of PHENIX

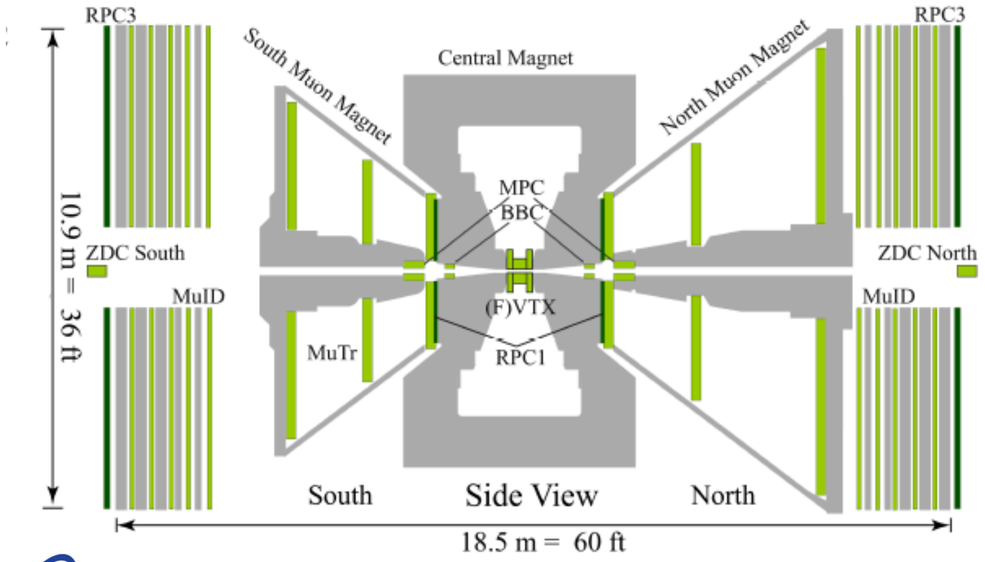

Studying semi-leptonic decay of heavy flavors with the muon arms

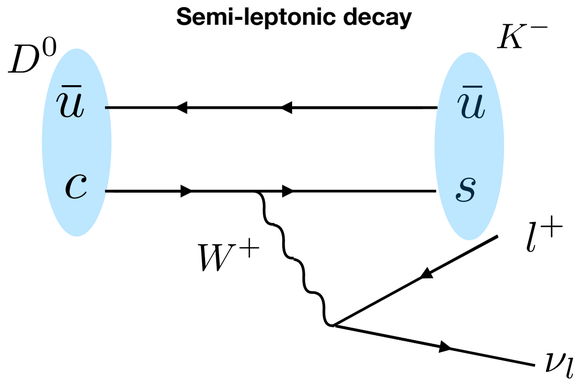

Muons from semi-leptonic decay of HF measured in muon arm in the forward/backward region of PHENIX

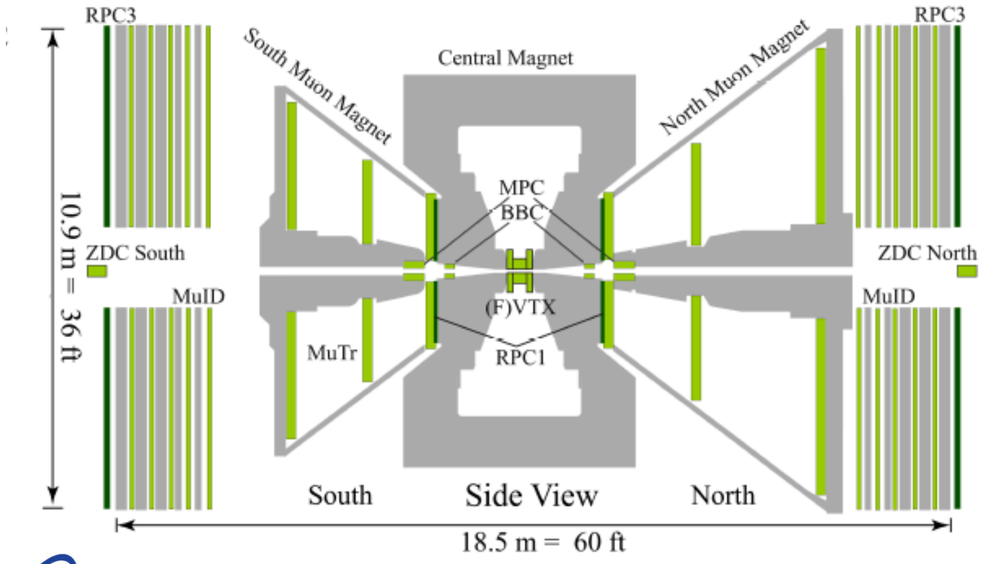

Particle	Lifetime $c\tau_0$
D^0	129.9 μm
D^+	311.8 μm
B^0	457.2 μm
B^+	491.1 μm

- Heavy flavor decays leave a displaced vertex signature.
- DCA_R (DCA along the radial projection of tracks) can be precisely determined with FVTX+VTX.

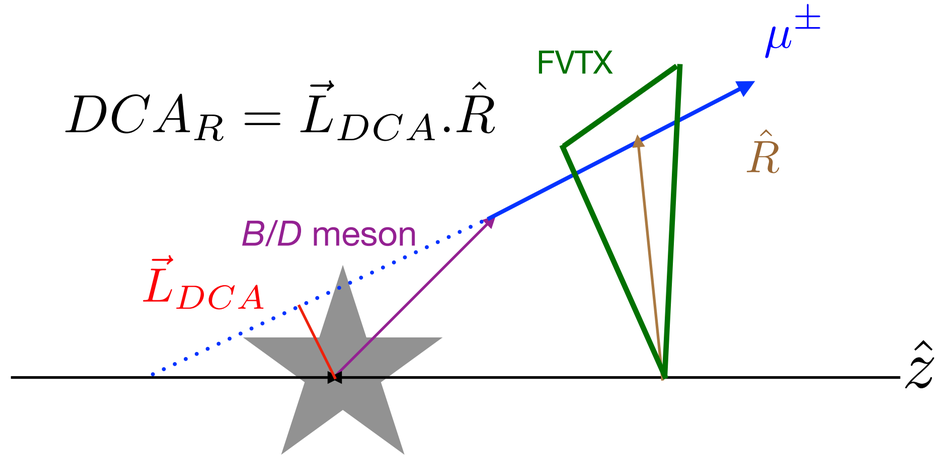

Supervised Machine Learning process

Input variables (**x**) for pythia embedded into data background

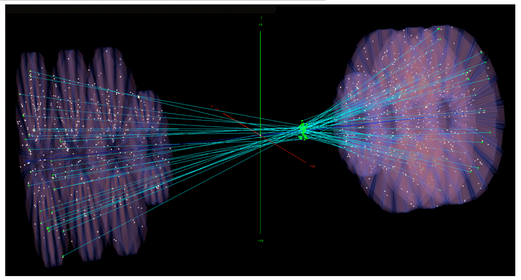

Training labeled data

Supervised Learning

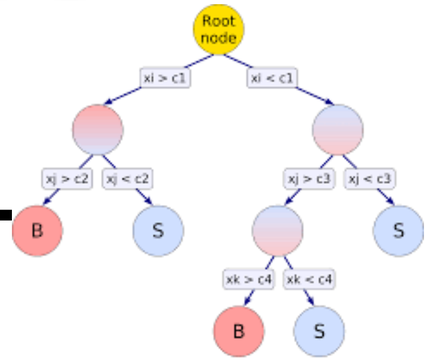

Known output

Input variables (**x**) for data

Mapping function f(**x**)

Output

DCA_R vs Machine Learning output

- Boosted Decision Tree (BDT) classifier is trained on multiple discriminating variables for more efficient classification.

- Input variable include:
  * DCA_R,
  * p_T,
  * η,
  * ϕ,
  * primary vertex,
  * primary vertex uncertainty,
  * distance between vertex & closest detector hit.

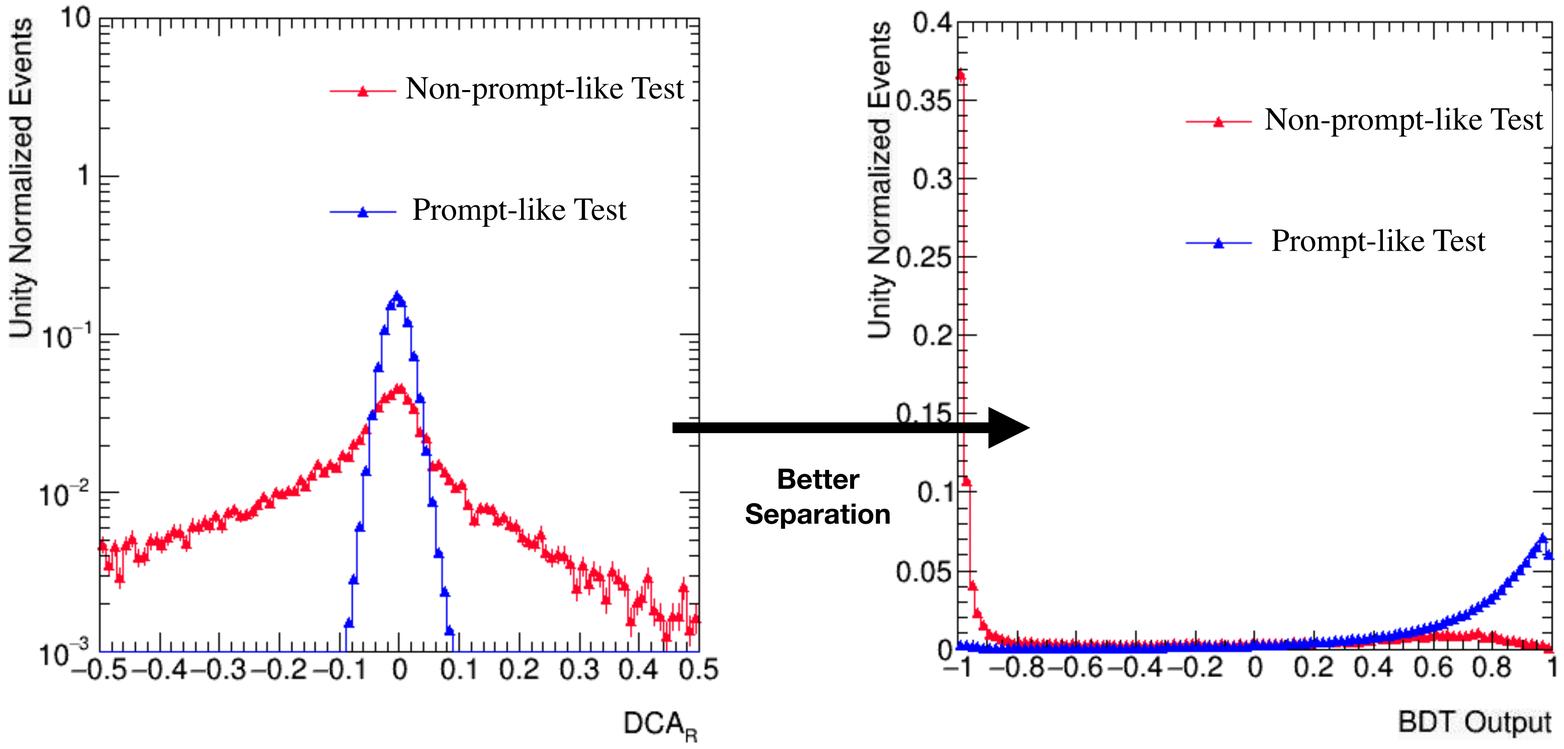

$K \rightarrow \mu$ simulation proxy for long decays (non-prompt-like) particles.

$J/\psi \rightarrow \mu$ simulation proxy for prompt-like particles.

Trained on two sources of background

DCA_R vs Machine Learning output

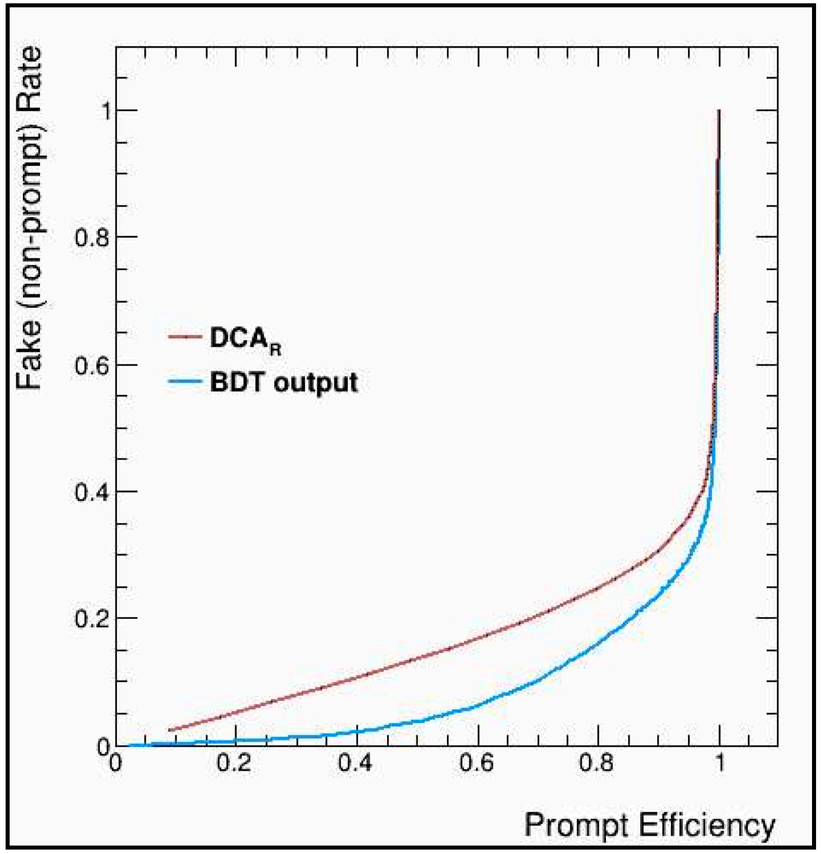

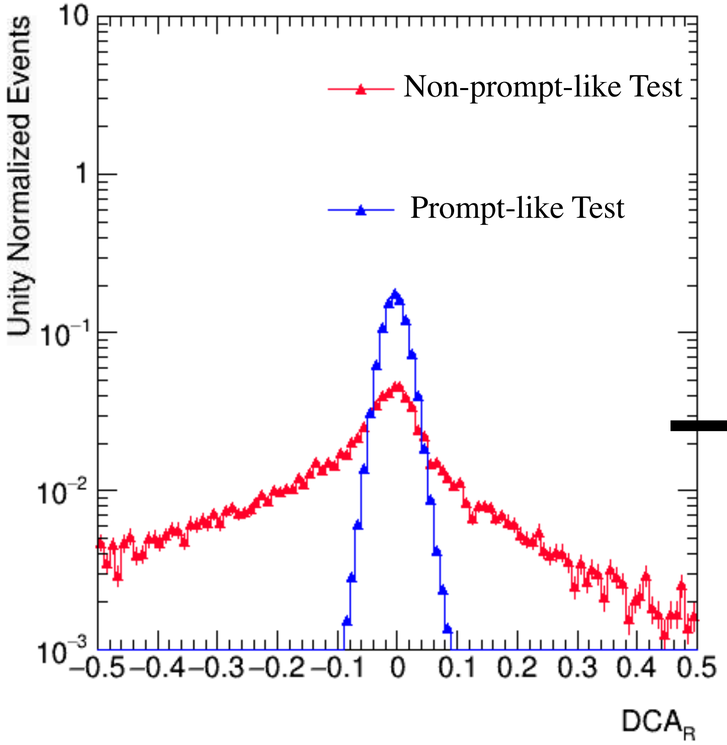

Better Separation

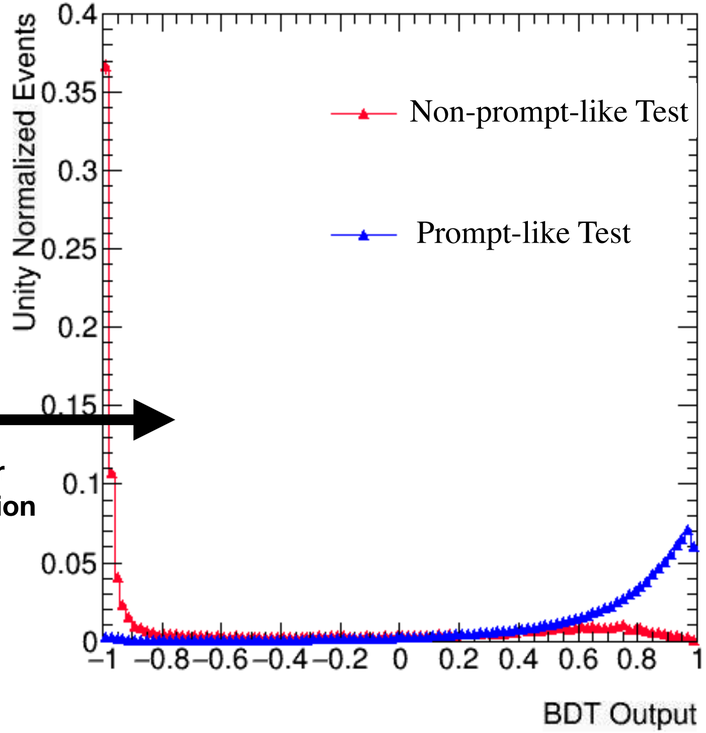

$K \rightarrow \mu$ simulation proxy for long decays (non-prompt-like) particles.

$J/\psi \rightarrow \mu$ simulation proxy for prompt-like particles.

Trained on two sources of background

Feasibility study of the c/b extraction using ML output

- Using the classification mapping function, ML output distribution is obtained for various background and heavy flavor muon signal processes.
- Pseudo data is generated using templates for signal and data.
- Signal proportion is varied, and feasibility of extracting the signal using ML output is studied.

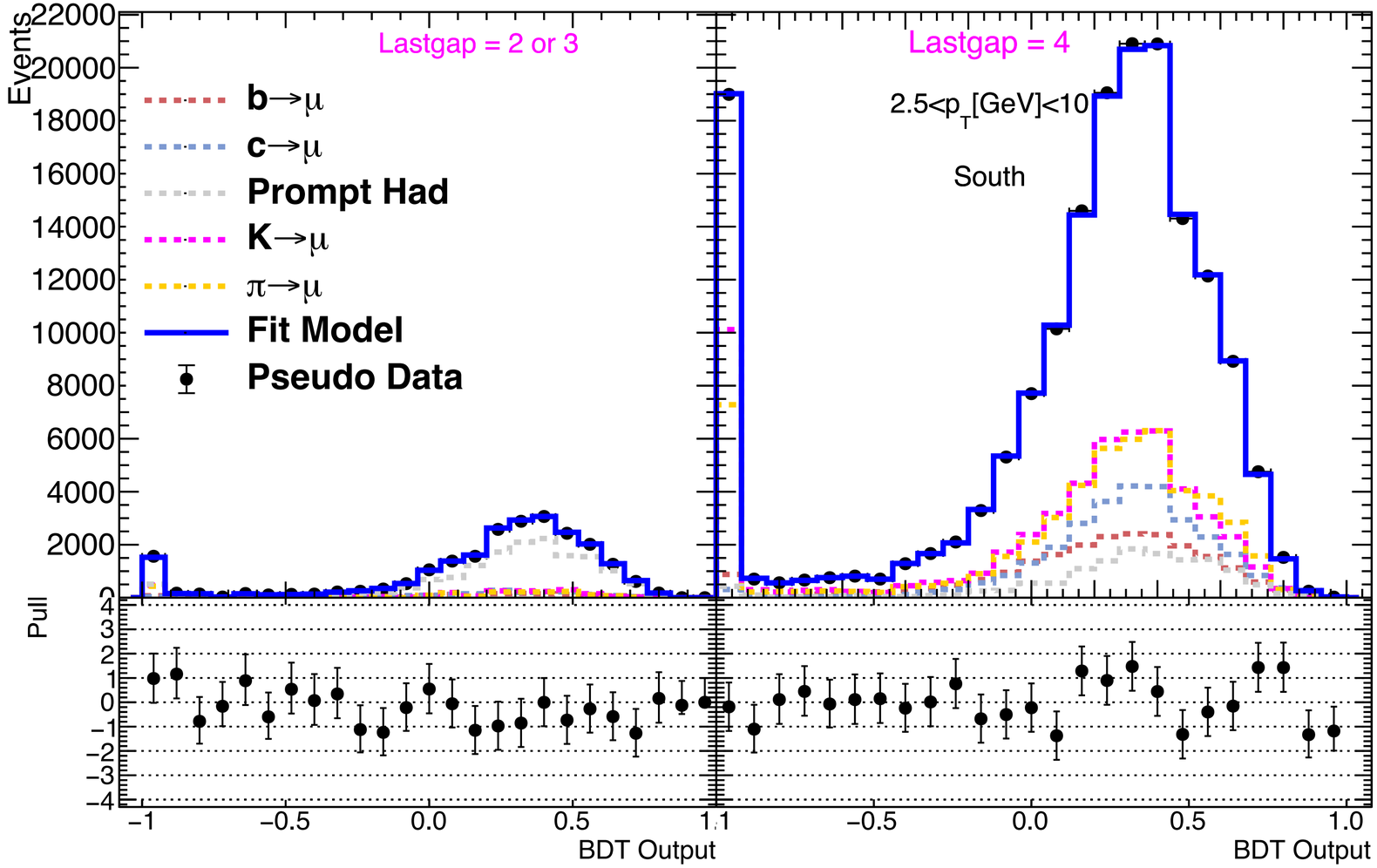

Feasibility study of the c/b extraction using ML output

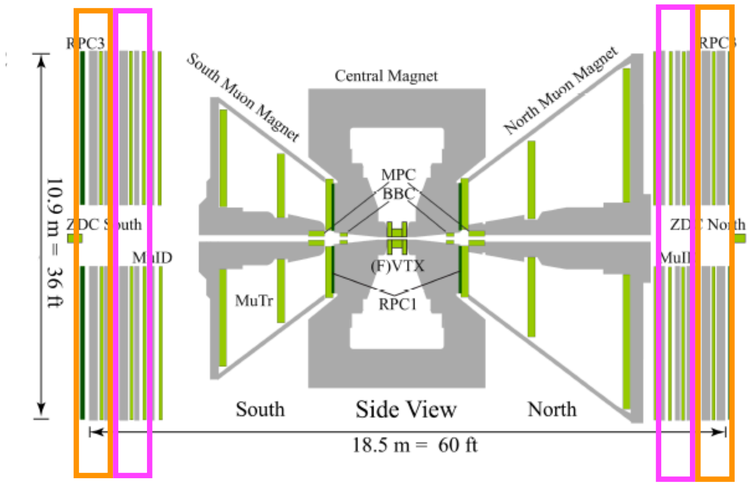

- Fitting is done simultaneously for tracks in prompt hadron & muon dominated region.
- Output b/(c+b) fraction agrees with the input within uncertainties for multiple input values.

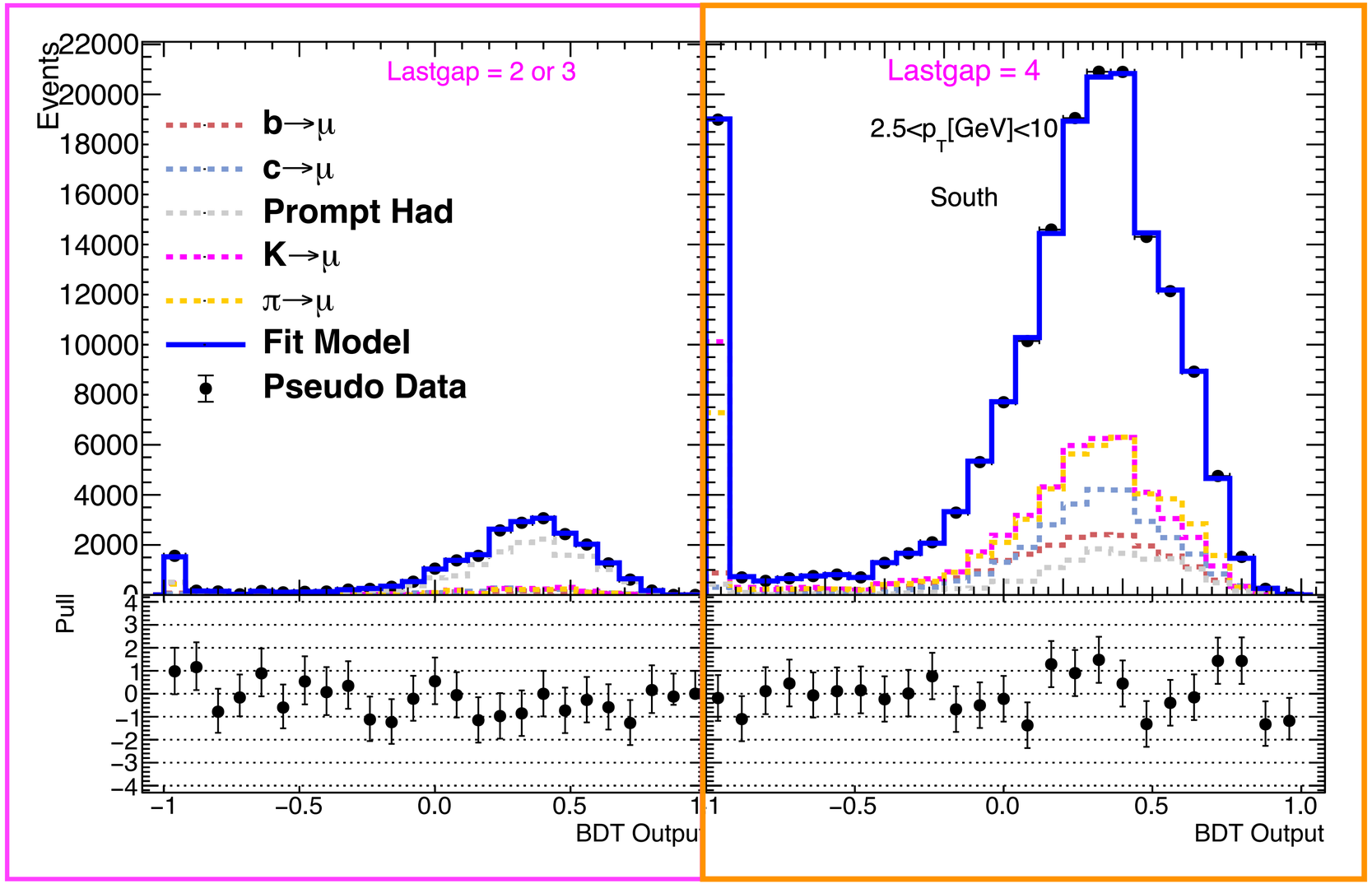

Outline

- Understanding gluon PDFs using photon+jet cross section measurement from the CMS pp data
- Heavy flavor “tagging”/classification using Machine Learning tools at PHENIX
- Unfolding development for top quark pair spin correlation and polarization at the CMS
- Other contributions to the CMS and PHENIX
- My interests in the EIC physics

Top quark pair spin correlation and polarization

Dilepton Channel

- Heaviest fundamental particle: m_t = 173.34±0.27(stat) ±0.71(syst) GeV [arXiv: 1403.4427].
- Short lifetime:

$$\frac{1}{m_t} < \frac{1}{\Gamma_t} < \frac{1}{\Lambda_{\mathrm{QCD}}} < \frac{m_t}{\Lambda^2}$$

production 10^{-27} s | lifetime 10^{-25} s | hadronization 10^{-24} s | spin flip 10^{-21} s

- In SM: Top quarks produced by strong interaction are mostly unpolarized but QCD causes top-quark spins to be correlated.
- In BSM scenarios: Resonances decaying to top can modify the correlation.

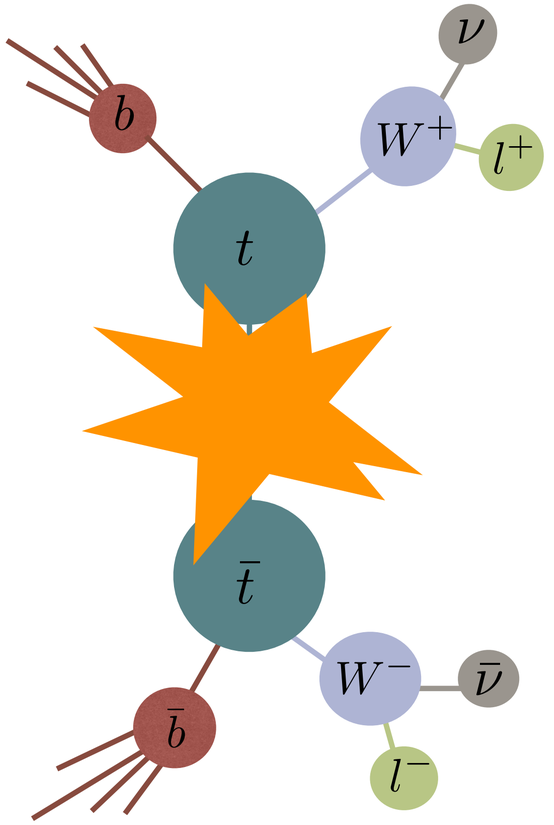

Decay products carry the top spin information.

We measured all the independent coefficients of the $t\bar{t}$ production spin density matrix

Unfolding in particle physics

true image

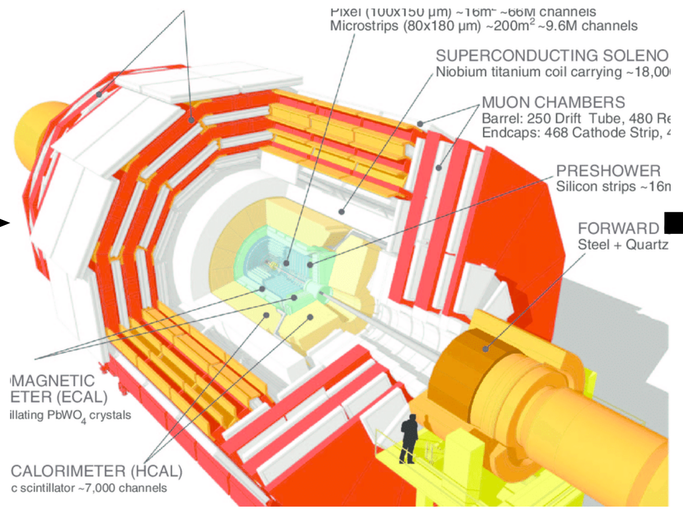

reconstructed image

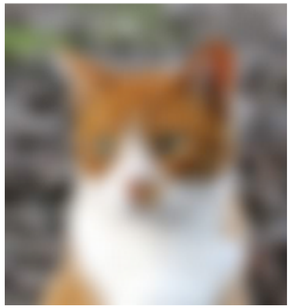

Unfolding procedure

unknown: estimate of true image

- Distributions measured by any detector are modified from the true underlying distribution due to its finite resolution and limited acceptance.

Unfolding in particle physics

true image

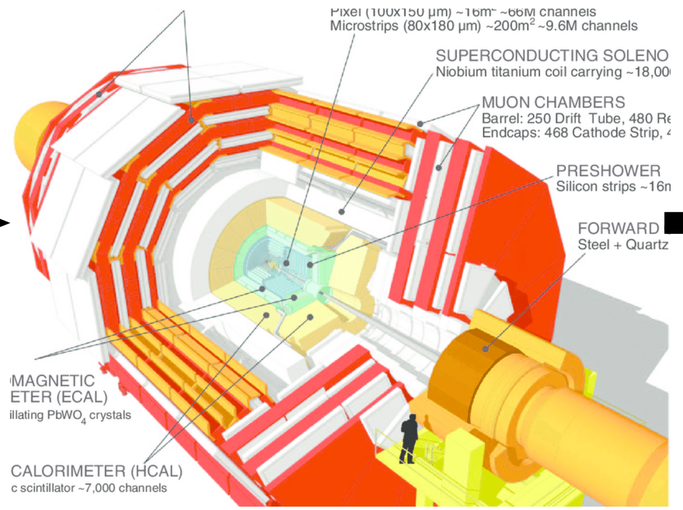

reconstructed image

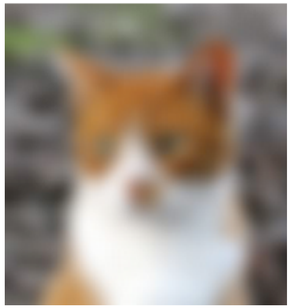

Unfolding procedure

unknown: estimate of true image

- Distributions measured by any detector are modified from the true underlying distribution due to its finite resolution and limited acceptance.
- In the top quark analysis major contribution to the smearing come from detector response, kinematic reconstruction algorithms, particle shower, and hadronization.
- These effects can be corrected from the reconstructed distributions using regularizaed unfolding method to retrieve the differential cross sections at parton level in the full phase space.

Regularized TUnfold method with no bias

$$\chi^2_{unf} = \chi^2_M + \tau^2 \chi^2_L + \lambda \sum_i (Mx - y)_i$$

Regularized TUnfold method with no bias

$$\chi^2_{unf} = \chi^2_M + \tau^2\chi^2_L + \lambda\sum_i (Mx - y)_i$$

$$\chi^2_M = (Mx - y)^T V_{yy}^{-1}(Mx - y)$$

Least sq. fit of re-folded output to the original data

Regularized TUnfold method with no bias

$$\chi^2_{unf} = \chi^2_M + \tau^2\chi^2_L + \lambda\sum_i (Mx - y)_i$$

$$\chi^2_M = (Mx - y)^T V_{yy}^{-1}(Mx - y)$$

$$\chi^2_L = (x - f * x_0)^T L^T L(x - f * x_0)$$

Least sq. fit of re-folded output to the original data

L matrix: Regularization term can be introduced to balance out negative correlation with positive correlation.

τ: Gives strength of regularization.

Regularization condition that minimizes the curvature of the vector ($x - f * x_0$) is used. Gives the difference between unfolded and the SM MC distributions where f is a normalization factor.

Regularized TUnfold method with no bias

$$\chi^2_{unf} = \chi^2_M + \tau^2\chi^2_L + \lambda\sum_i (Mx - y)_i$$

$$\chi^2_M = (Mx - y)^T V^{-1}_{yy}(Mx - y)$$

$$\chi^2_L = (x - f * x_0)^T L^T L(x - f * x_0)$$

Least sq. fit of re-folded output to the original data

L matrix: Regularization term can be introduced to balance out negative correlation with positive correlation.

τ: Gives strength of regularization.

Regularization condition that minimizes the curvature of the vector ($x - f * x_0$) is used. Gives the difference between unfolded and the SM MC distributions where f is a normalization factor.

Constraint to ensure area of refolded output matches the input data

Optimization of regularization strength

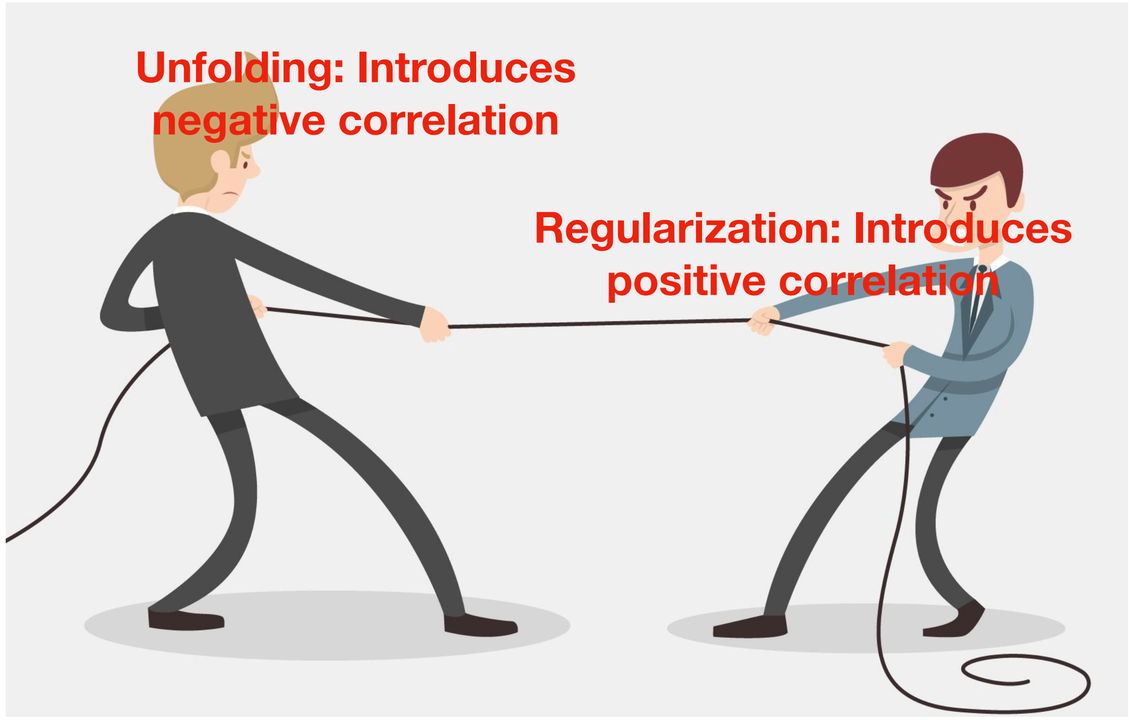

Name of the game is push and pull between matrix inversion and regularization

Tune regularization strength to minimize the average global correlation

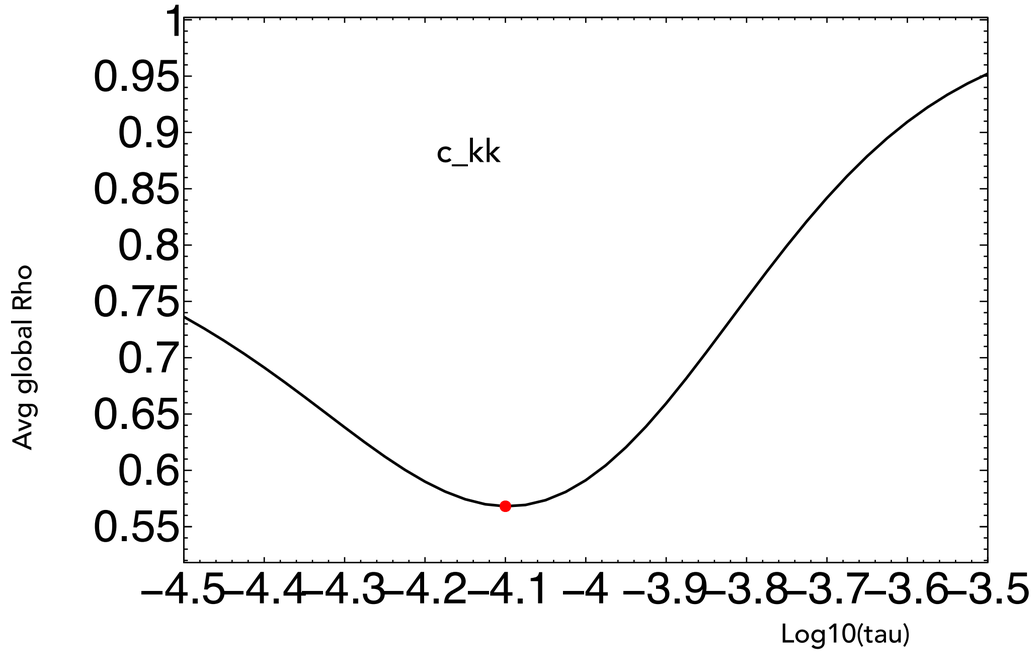

- Larger tau will result in unfolded result close to the bias distribution (gen-level MC).
- Smaller tau results in larger statistical fluctuations.

Regularization bias

- When new physics is present we expect the spin coefficients will change.
- Except when ($x - f * x_0$) is linear, regularization will cause bias in the values of spin observables because the curvature is non zero.

Regularization bias

- When new physics is present we expect the spin coefficients will change.
- Except when ($x - f * x_0$) is linear, regularization will cause bias in the values of spin observables because the curvature is non zero.
- Unique “Bin Factor Function” (BFF) are computed for different spin observables to ensure regularizing the curvature is unbiased in the presence of a new physics.
- Test of “linearity” i.e. lack of regularization bias by injecting 20 different values of coefficients that differ from SM prediction by +/-0.5.

Slope of linearity plot (for each bin)

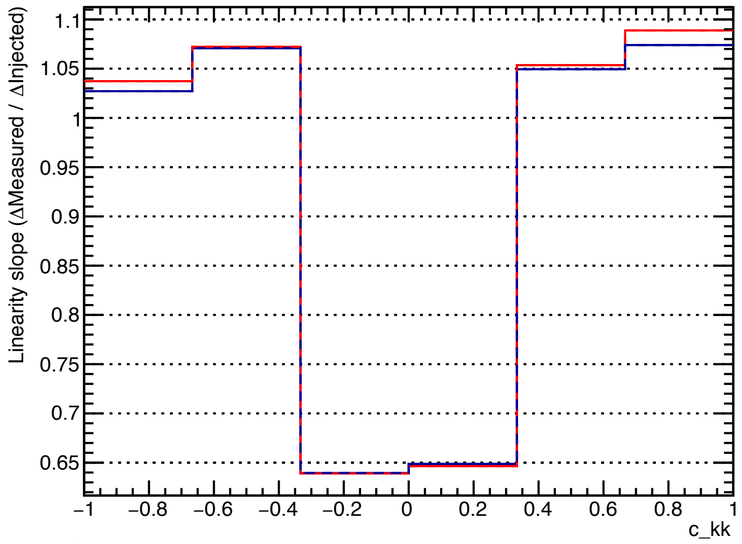

Slope of linearity plot (for each bin)

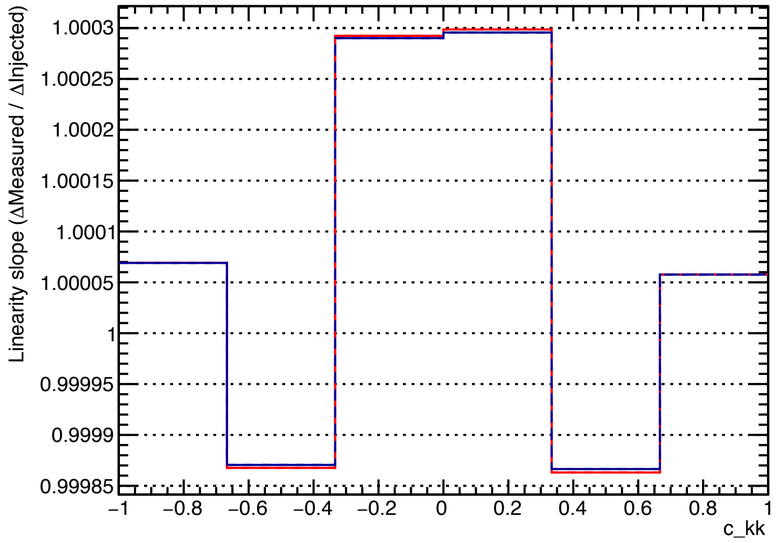

For unbiased measurement, slope of linearity plot = 1

Regularization bias

- When new physics is present we expect the spin coefficients will change.
- Except when (x -f * x_0) is linear, regularization will cause bias in the values of spin observables because the curvature is non zero.
- Unique “Bin Factor Function” (BFF) are computed for different spin observables to ensure regularizing the curvature is unbiased in the presence of a new physics.
- Test of “linearity” i.e. lack of regularization bias by injecting 20 different values of coefficients that differ from SM prediction by +/-0.5.

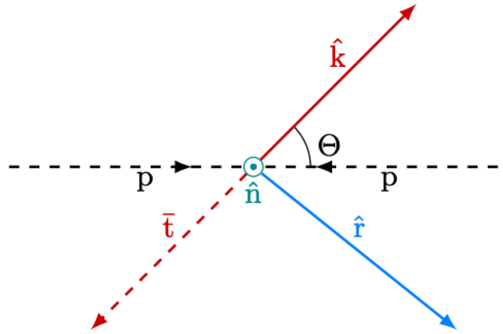

Slope of linearity plot (for each bin)

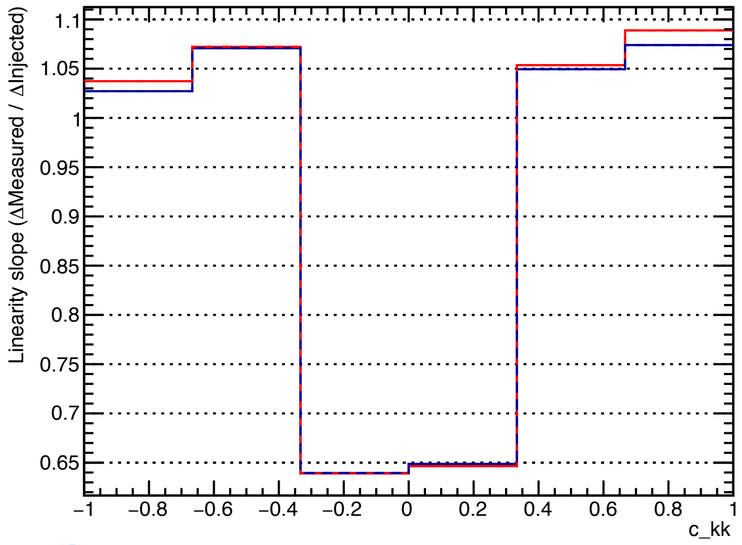

Slope of linearity plot (for each bin)

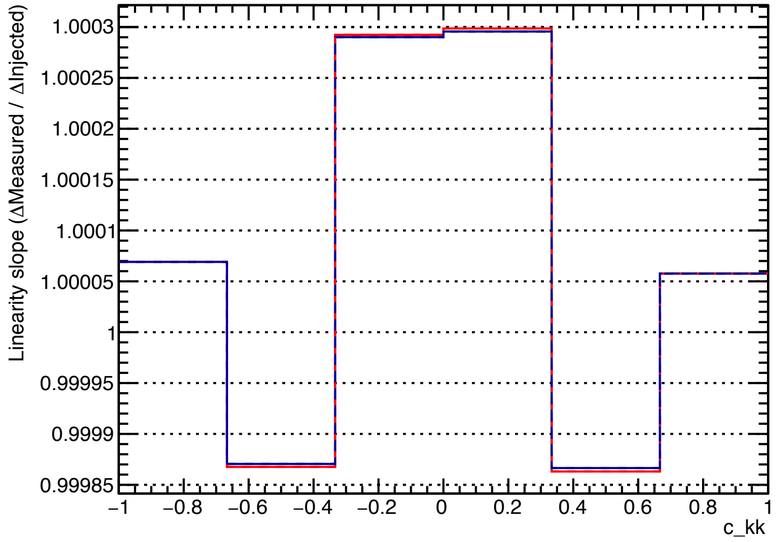

c_kk: spin correlation coefficient in the direction of top in $t\bar{t}$ zero momentum frame.

Generated by P- and CP- conserving interactions.

For unbiased measurement, slope of linearity plot = 1

Unfolded distribution example

Coefficient	Measured	POWHEGv2	MG5_aMC@NLO	NLO calculation
C_{kk}	0.300 ± 0.038	$0.314\ ^{+0.005}_{-0.004}$	$0.325\ ^{+0.011}_{-0.006}$	$0.331\ ^{+0.002}_{-0.002}$

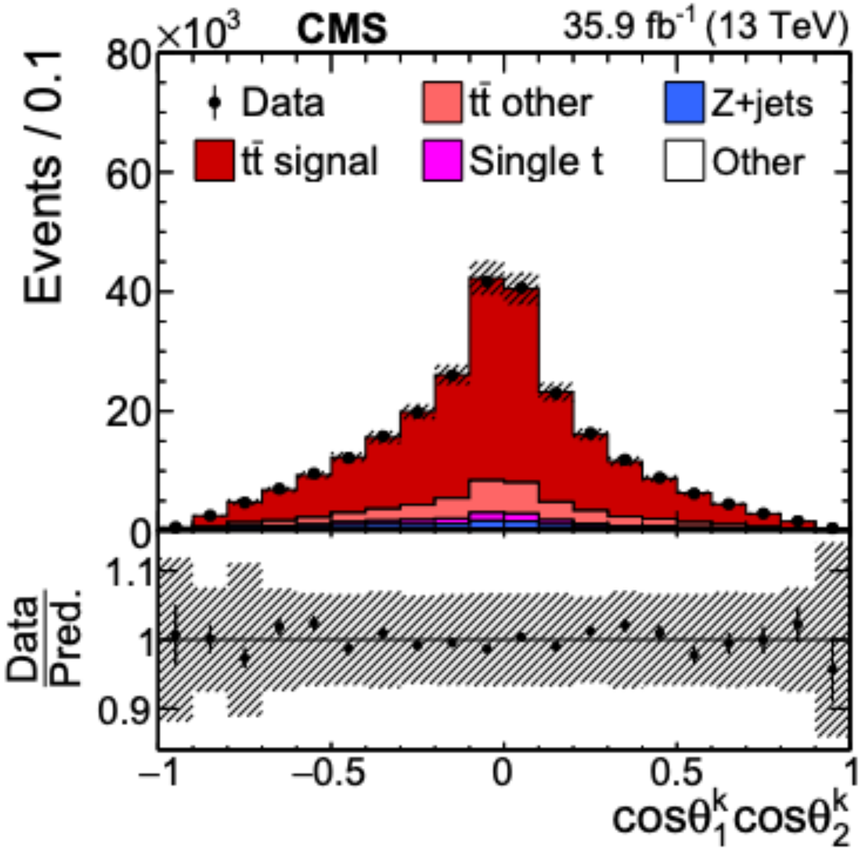

reconstructed yield

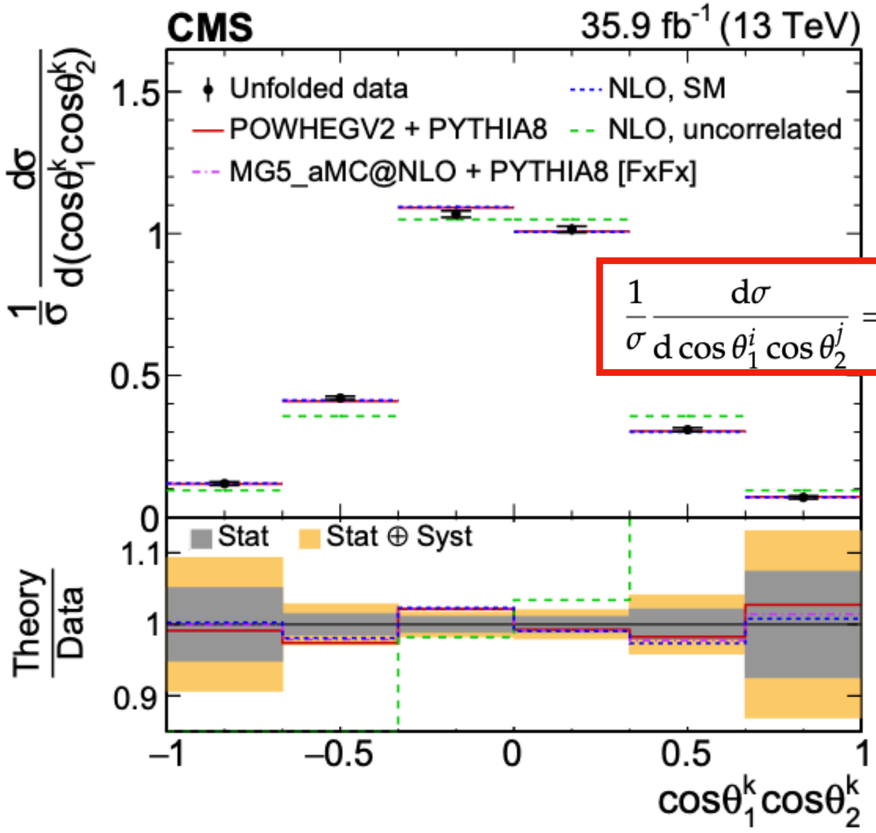

unfolded cross section

$$\frac{1}{\sigma}\frac{\mathrm{d}\sigma}{\mathrm{d}\cos\theta_1^i \cos\theta_2^j} = \frac{1}{2}\left(1 - C_{ij}\cos\theta_1^i \cos\theta_2^j\right) \ln\left(\frac{1}{|\cos\theta_1^i \cos\theta_2^j|}\right)$$

Phys. Rev. D 100, 072002 (2019)

← **distribution related to the c_kk coefficient**

Outline

- Understanding gluon PDFs using photon+jet cross section measurement from the CMS pp data
- Heavy flavor “tagging”/classification using Machine Learning tools at PHENIX
- Unfolding development for top quark pair spin correlation and polarization at the CMS
- Other contributions to the CMS and PHENIX
- My interests in the EIC physics

Other contributions not mentioned in detail

- Optimization of algorithm used for mitigating spikes (anomalous signals observed in the CMS-ECAL from direct ionization of avalanche photodiodes).

- Photon identification performance studies with the Eγ Physics Object Group at the CMS.

- Code development for the CMS Pixel Data Quality Monitoring.

- Mechanical assembly of the forward pixel detector for Phase I upgrade of the CMS detector.

- Starting the study of transverse and longitudinal spin asymmetries using the correlations of tracks measured by the muon tracker and FVTX detectors at PHENIX experiment.

- Various mentoring, outreach, and teaching activities….etc.

Outline

- Understanding gluon PDFs using photon+jet cross section measurement from the CMS pp data
- Heavy flavor “tagging”/classification using Machine Learning tools at PHENIX
- Unfolding development for top quark pair spin correlation and polarization at the CMS
- Other contributions to the CMS and PHENIX
- My interests in the EIC physics

EIC efforts of interest

- DIS jet production can provide access to flavor separated probe of pQCD.
- In eA collisions, it can probe initial/final state cold nuclear matter effects.
- I've experience with particle flow jets at the CMS.
- I have experience with HF tagging using ML.
- I have experience with regularized unfolding methods to correct for detector effects that would be applicable at EIC.

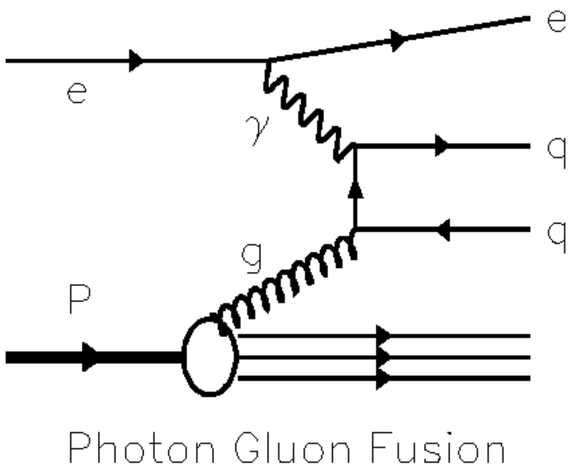

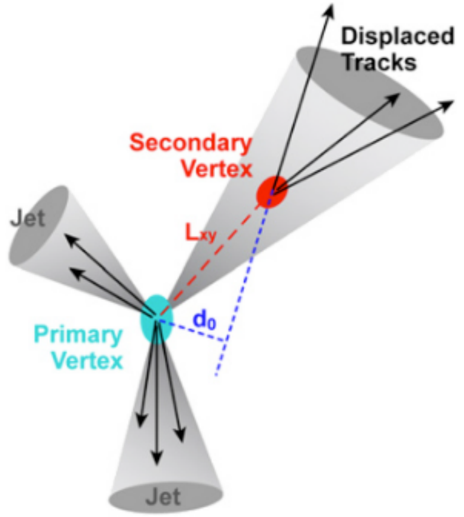

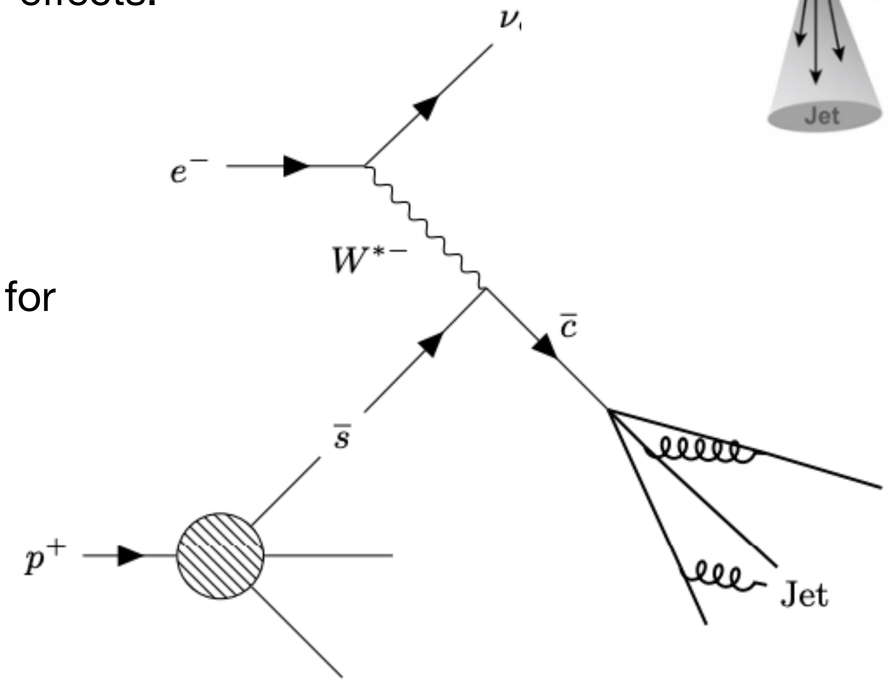

HF tagging

LO diagram for the production of charm in CC electron-proton DIS @ EIC

Summary

- Led two major HEP analyses by CMS in photon+jet and top quark.
- Leading efforts on the study of charm/bottom separated study of single muons in the Heavy Ion program at PHENIX.
- Experience in advanced statistical tools, such as unfolding and ML.
- Experience in MC and data analysis.
- Have taken relevant courses and some experience on detector work.
- Diverse experiences in different high energy/nuclear physics projects, including a project aimed towards stockpile stewardship.
- Enjoys working with jets.

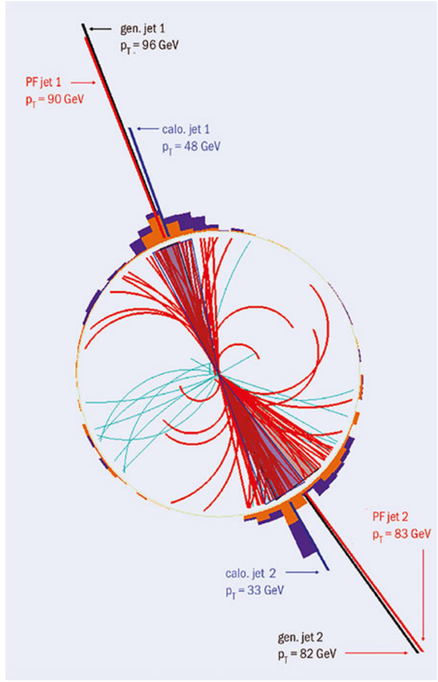

Thanks!

Additional Materials

QCD

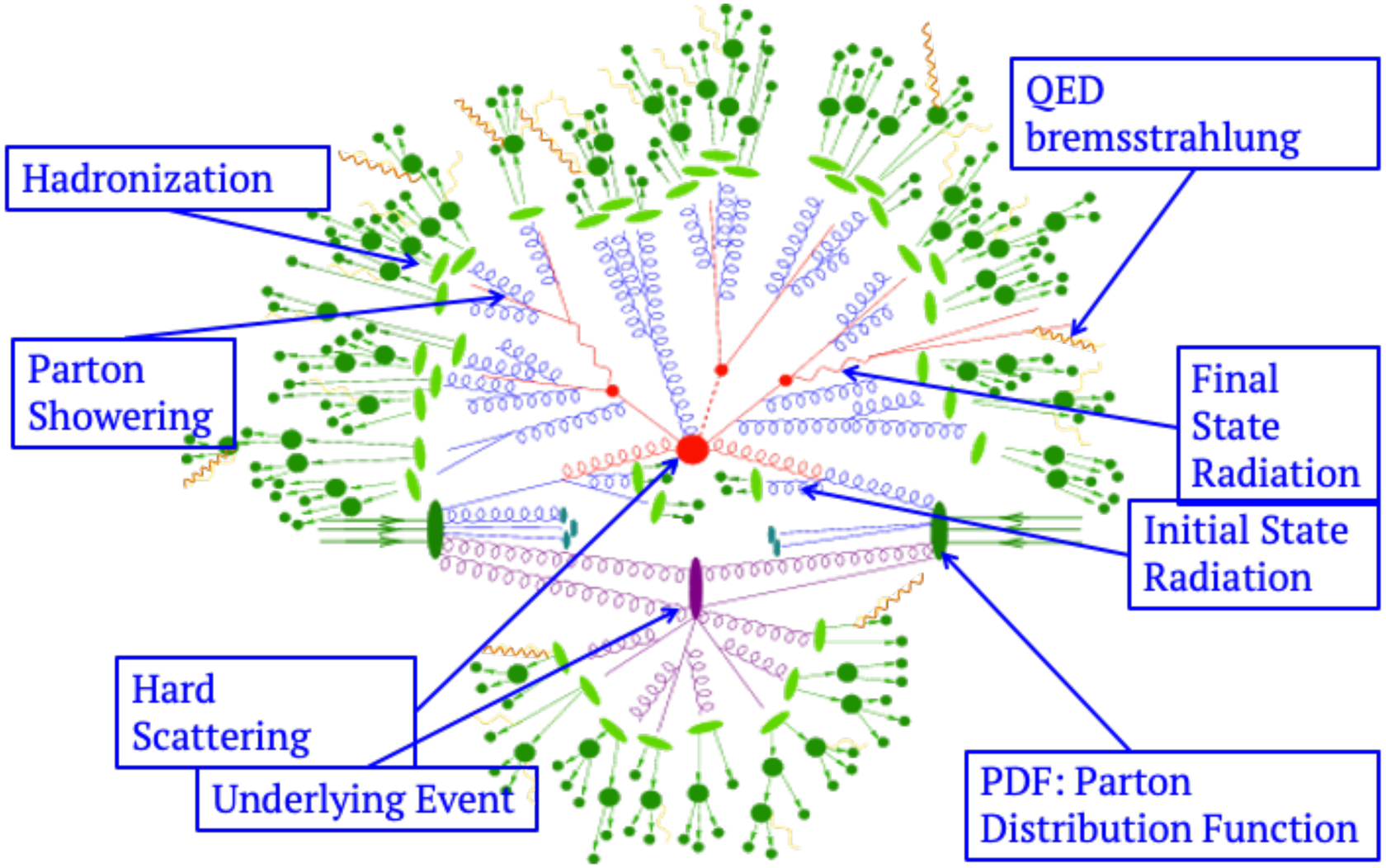
Hadronization
Parton Showering
QED bremsstrahlung
Final State Radiation
Initial State Radiation
Hard Scattering
Underlying Event
PDF: Parton Distribution Function

CMS

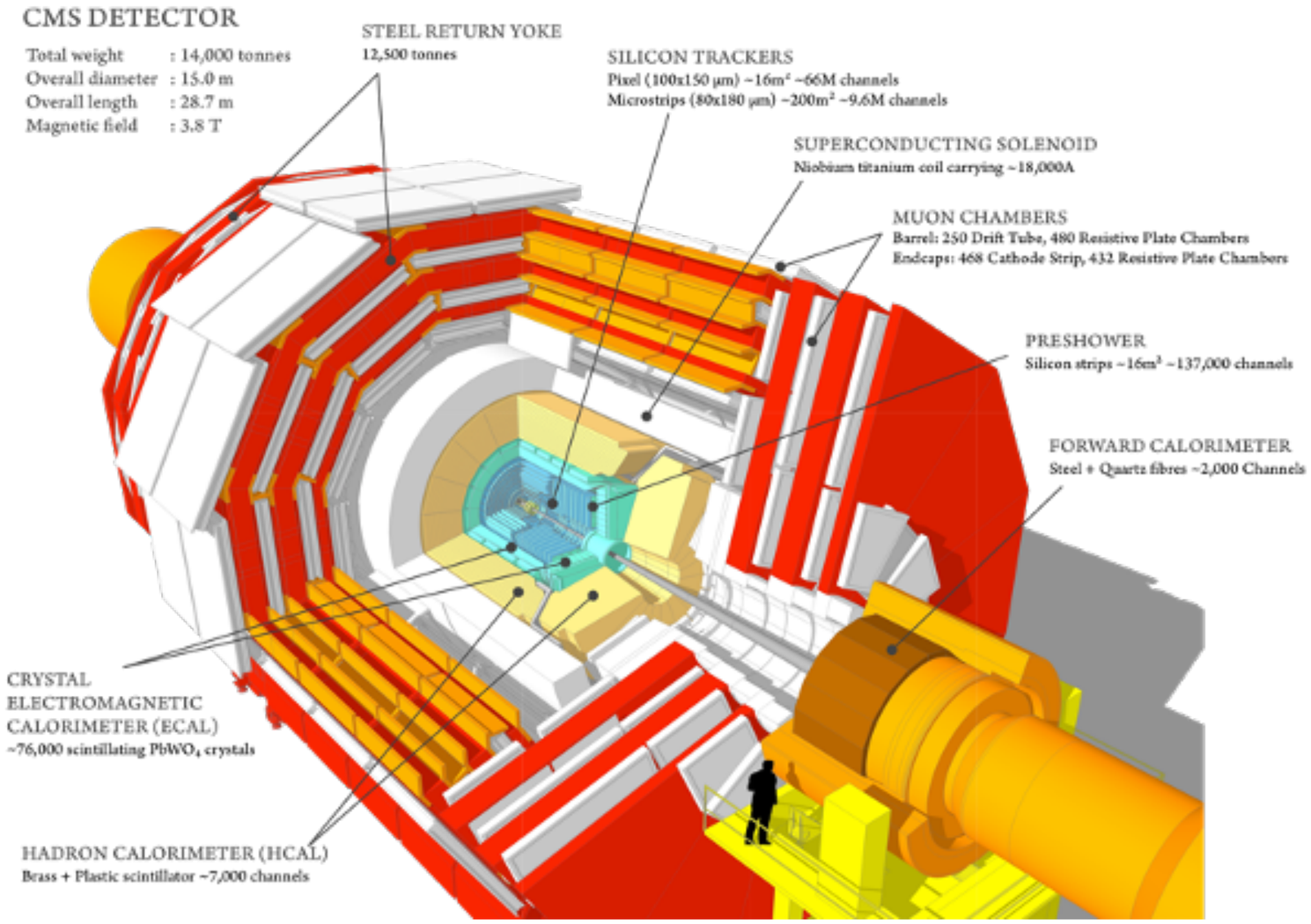
CMS DETECTOR
Total weight : 14,000 tonnes
Overall diameter : 15.0 m
Overall length : 28.7 m
Magnetic field : 3.8 T
STEEL RETURN YOKE
12,500 tonnes
SILICON TRACKERS
Pixel (100x150 μm) ~16m² ~66M channels
Microstrips (80x180 μm) ~200m² ~9.6M channels
SUPERCONDUCTING SOLENOID
Niobium titanium coil carrying ~18,000A
MUON CHAMBERS
Barrel: 250 Drift Tube, 480 Resistive Plate Chambers
Endcaps: 468 Cathode Strip, 432 Resistive Plate Chambers
PRESHOWER
Silicon strips ~16m² ~137,000 channels
FORWARD CALORIMETER
Steel + Quartz fibres ~2,000 Channels
CRYSTAL ELECTROMAGNETIC CALORIMETER (ECAL)
~76,000 scintillating $PbWO_4$ crystals
HADRON CALORIMETER (HCAL)
Brass + Plastic scintillator ~7,000 channels

CMS ECAL

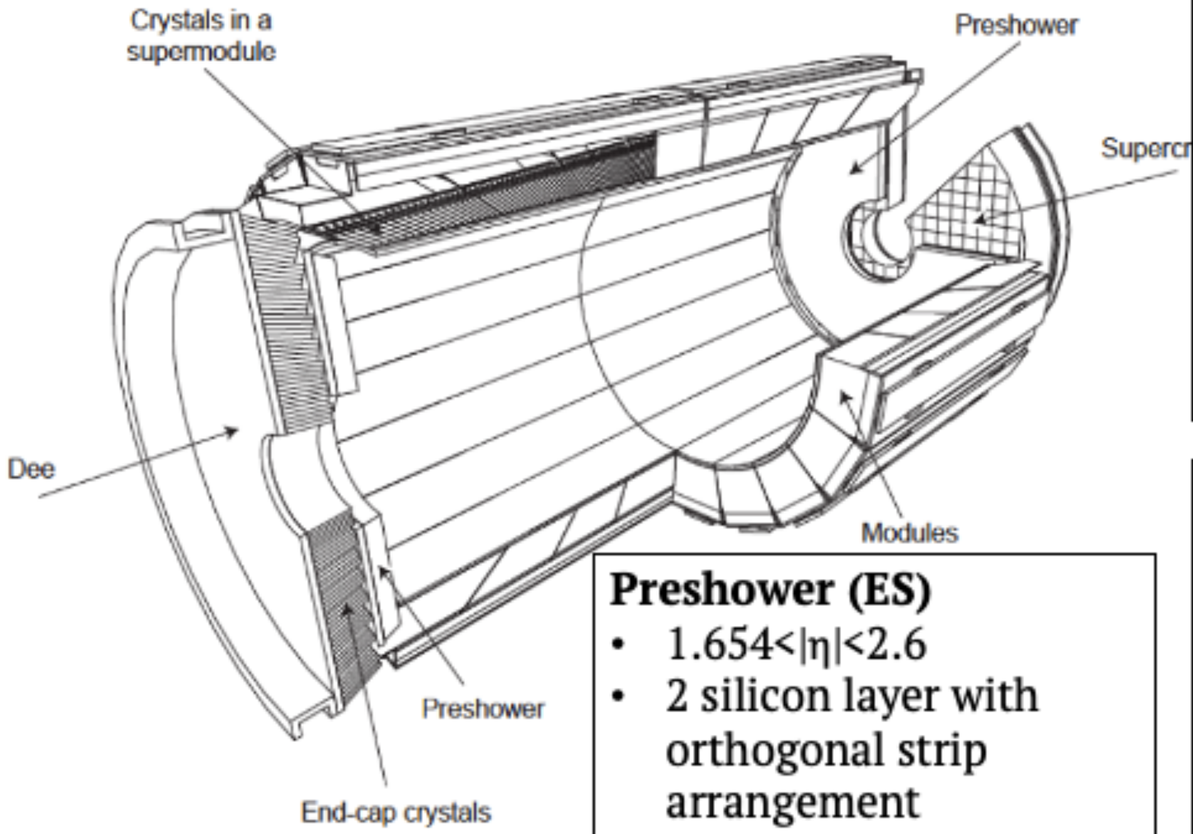

Barrel (EB)
- $|\eta|<1.44$
- 61,200 Lead tungstate ($PbWO_4$) crystals
- Photodetector: Avalanche Photodiodes (APDs)
- Crystal front face: 0.0174 X 0.0174 in η-ϕ

Preshower (ES)
- $1.654<|\eta|<2.6$
- 2 silicon layer with orthogonal strip arrangement
- Provides extra spatial resolution to the EEs

Endcaps (EE)
- $1.56<|\eta|<3.0$
- 15,000 $PbWO_4$ crystals
- Photodetector: Vacuum Phototriodes (VPTs)
- Crystal granularity varies from 0.0175 X 0.0175 to 0.05 X 0.05 in η-ϕ

CMS ECAL

- $PbWO_4$ has short radiation length X_0= 0.89 cm.
- Moliere radius (radius of a cylinder containing ~ 90% of electron shower's energy) = 2.2 cm.
- High density of 8.3 g/cm^3.
- Emits scintillation light proportional to the interacting particles energy.
- Almost 80% of the scintillation light is emitted within the 25 ns of nominal LHC bunch crossing.

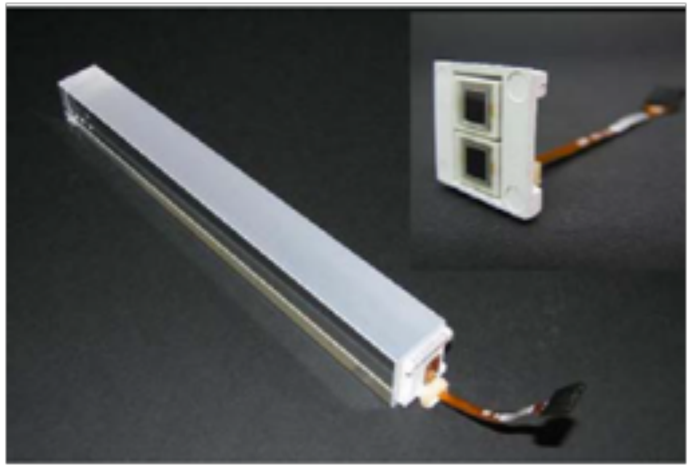

EB crystal with APD

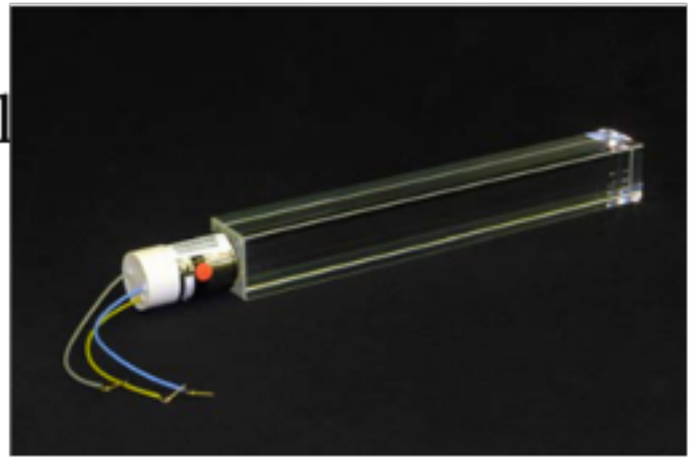

EE crystal with VPT

Measurement of $t\bar{t}$ Spin Density Matrix

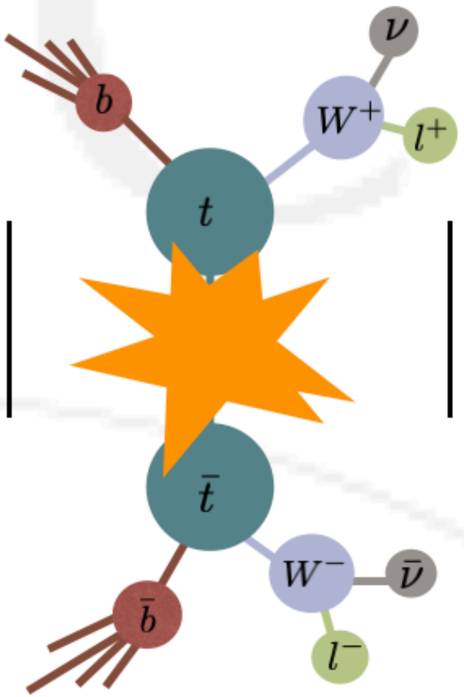

- Decompose $t\bar{t}$ production and analyze all the spin correlation and polarization coefficients simultaneously. [JHEP12(2015)026]

$$\propto A\mathbb{I}\times\mathbb{I}+B_i^+\sigma^i\times\mathbb{I}+B_i^-\sigma^i\times\mathbb{I}+C_{ij}\sigma^i\times\sigma^j$$

- B_i and C_{ij} are further decomposed in terms of orthonormal basis ($\hat{k}/\hat{p}$: direction of top/incoming parton in $t\bar{t}$ ZMF):

$$\{\hat{\mathbf{r}},\hat{\mathbf{k}},\hat{\mathbf{n}}\}: \quad \hat{\mathbf{r}}=\frac{1}{r}(\hat{\mathbf{p}}-y\hat{\mathbf{k}}), \quad \hat{\mathbf{n}}=\frac{1}{r}(\hat{\mathbf{p}}\times\hat{\mathbf{k}}), \quad y=\hat{\mathbf{k}}\cdot\hat{\mathbf{p}}, \quad r=\sqrt{1-y^2}.$$

$$\tilde{B}_i^{I\pm}=b_r^{I\pm}\hat{r}_i+b_k^{I\pm}\hat{k}_i+b_n^{I\pm}\hat{n}_i\,,$$

$$\begin{aligned}\tilde{C}_{ij}^{I}=&\,c_{rr}^{I}\hat{r}_i\hat{r}_j+c_{kk}^{I}\hat{k}_i\hat{k}_j+c_{nn}^{I}\hat{n}_i\hat{n}_j\\&+c_{rk}^{I}(\hat{r}_i\hat{k}_j+\hat{k}_i\hat{r}_j)+c_{kn}^{I}(\hat{k}_i\hat{n}_j+\hat{n}_i\hat{k}_j)+c_{rn}^{I}(\hat{r}_i\hat{n}_j+\hat{n}_i\hat{r}_j)\\&+\epsilon_{ijl}(c_r^{I}\hat{r}_l+c_k^{I}\hat{k}_l+c_n^{I}\hat{n}_l)\,.\end{aligned}$$

CP odd, P odd
CP even, P even
CP even, P odd
CP odd, P even

Observables

- Using the reference axis from before, angular distribution of two leptons is measured in its parents reference frame is given by,

$$\frac{1}{\sigma}\frac{d\sigma}{d\cos\theta_1^i d\cos\theta_2^j} = \frac{1}{4}\left(1 + B_1(i)\cos\theta_1^i + B_2(j)\cos\theta_2^j - C(i,j)\cos\theta_1^i\cos\theta_2^j\right)$$

- Single differential cross section are given by,

$$\frac{1}{\sigma}\frac{d\sigma}{d\cos\theta_1^i} = \frac{1}{2}\left(1 + B_1(i)\cos\theta_1^i\right)$$

$$\frac{1}{\sigma}\frac{d\sigma}{d\cos\theta_2^i} = \frac{1}{2}\left(1 + B_2(i)\cos\theta_2^i\right)$$

$$\frac{1}{\sigma}\frac{d\sigma}{d\cos\theta_1^i\cos\theta_2^j} = \frac{1}{2}\left(1 - C(i,j)\cos\theta_1^i\cos\theta_2^j\right)\log\left(\frac{1}{\left|\cos\theta_1^i\cos\theta_2^j\right|}\right)$$

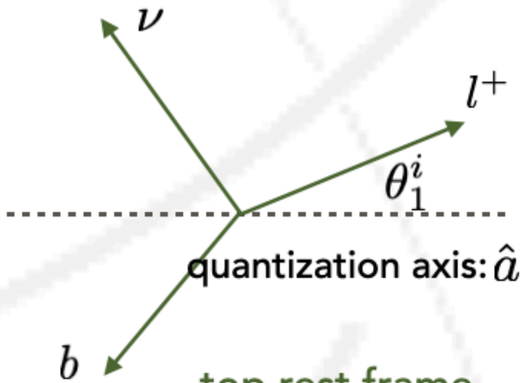

Response Distribution

- Measured distributions after background subtraction can be expressed in terms of underlying parton-level distributions.

measured distribution → $\vec{y} = M\vec{x}$ ← parton-level distribution

response matrix → $\vec{y} = M\vec{x}$

- M describes probability for an event produced in bin i to be measured in bin j.
- M is modeled using nominal $t\bar{t}$ sample.

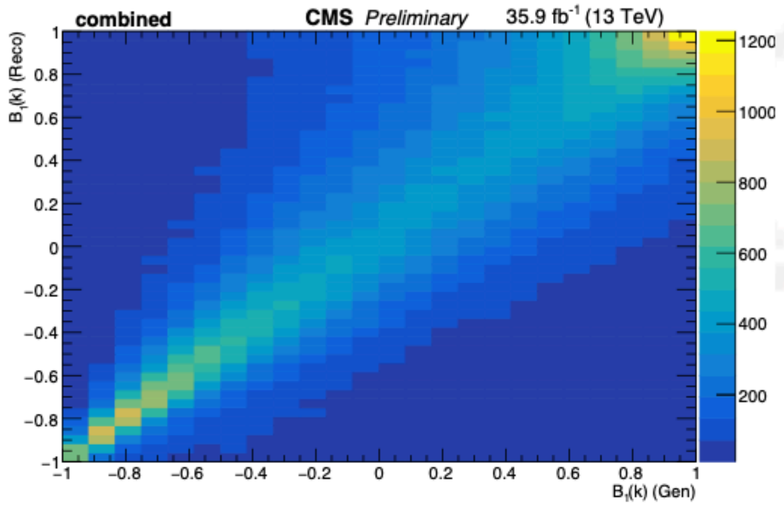

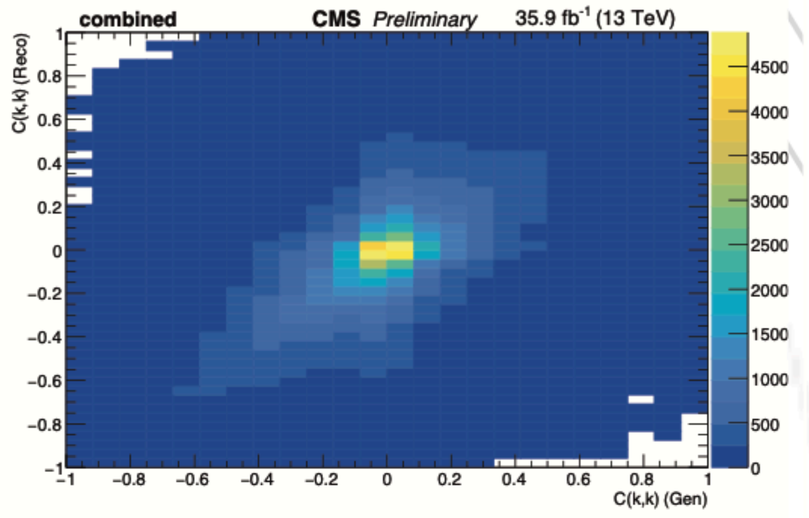

Systematic Uncertainty

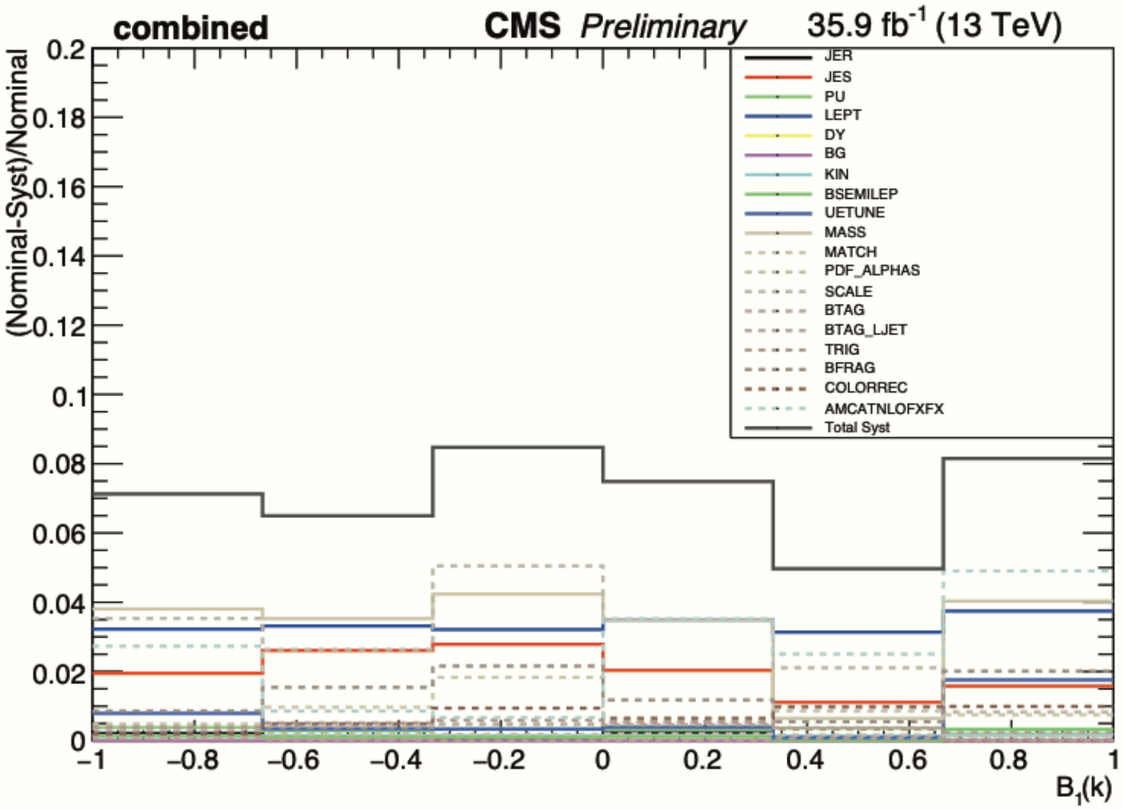

The results returned by TUnfoldDensity have been validated using the traditional method on 2015 dataset.

- Response matrices are filled from MC for each systematics.
- Traditionally data would be unfolded with the response matrices corresponding to each systematics and subtracted from nominal unfolded distribution.
- With TUnfoldDensity we can provide all the alternative response matrices at once, and obtain the unfolded (Nominal - Syst) distributions.

f_{SM}

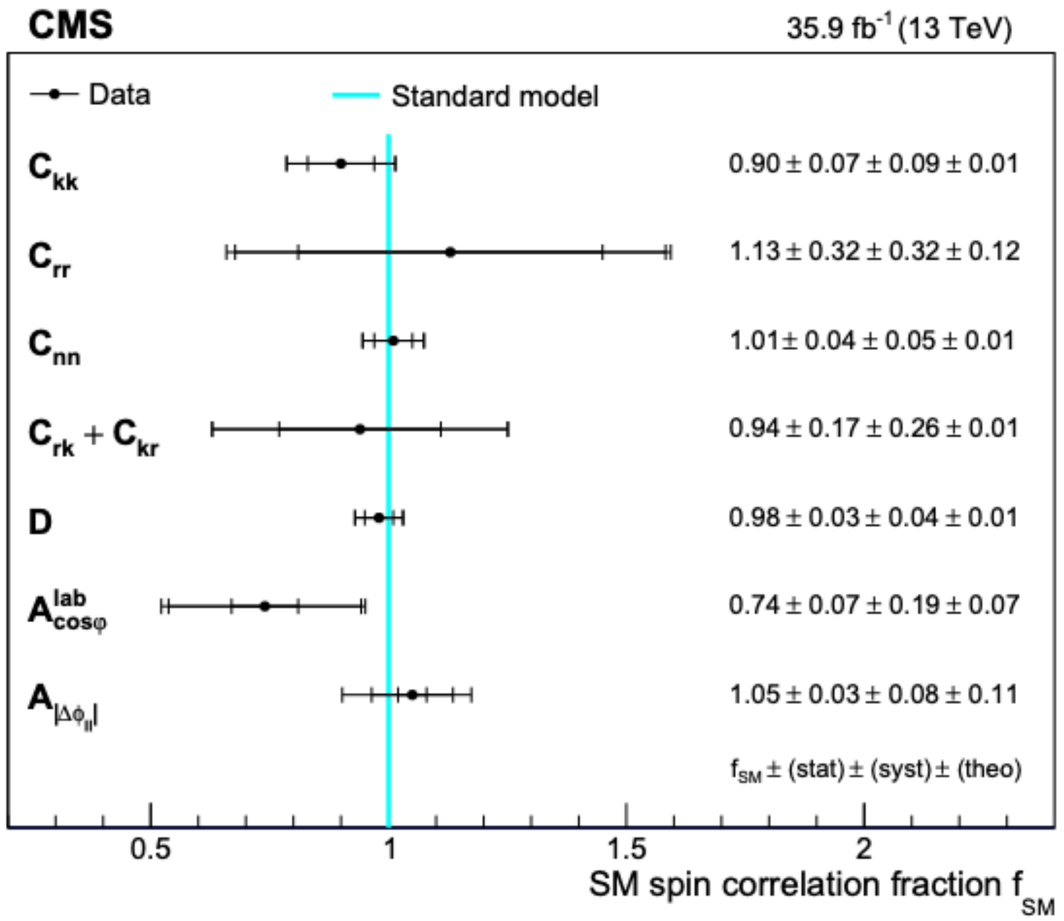

Figure 13: Measured values of f_{SM}, the strength of the measured spin correlations relative to the SM prediction. The inner vertical bars give the statistical uncertainty, the middle bars the total experimental uncertainty (statistical and systematic), and the outer bars the total uncertainty. The numerical measured values with their uncertainties are given on the right.

Constrain on Wilson coefficient that is related to the operator that results in top quark CMDM in the EFT framework

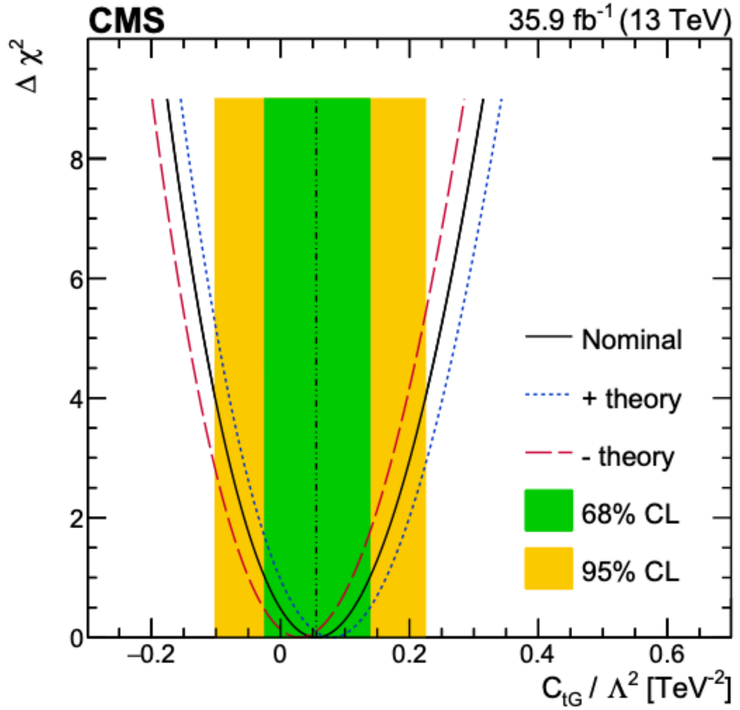

Figure 14: The $\Delta\chi^2$ values from the fit to the data as a function of C_{tG}/Λ^2. The solid line is the result of the nominal fit, and the dotted and dashed lines show the most-positive and most-negative shifts in the best fit C_{tG}/Λ^2, respectively, when the theoretical inputs are allowed to vary within their uncertainties. The vertical line denotes the best fit value from the nominal fit, and the inner and outer areas indicate the 68 and 95% CL, respectively.

Heavy Flavor production at PHENIX forward rapidity

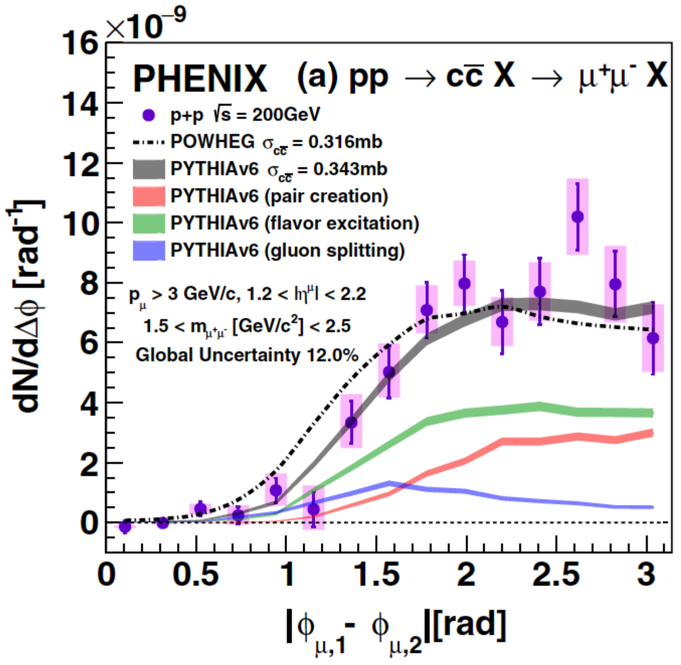

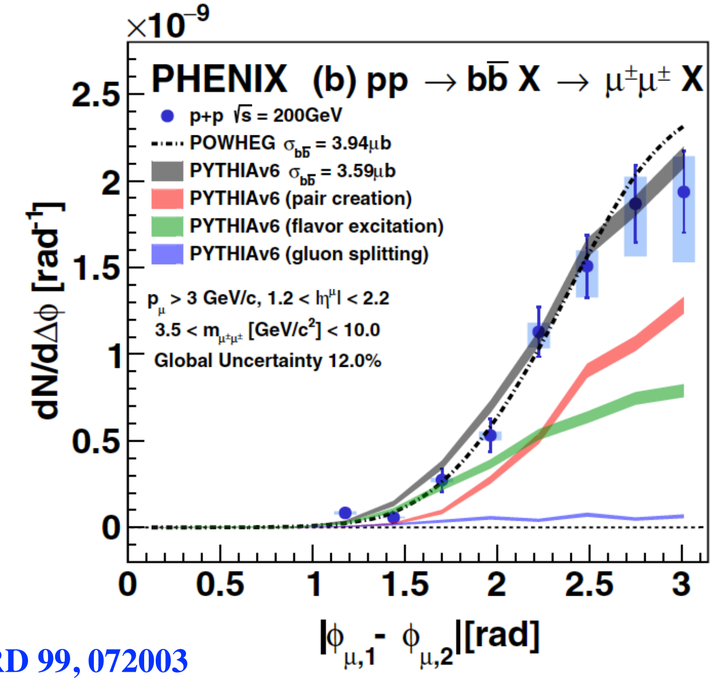

PRD 99, 072003

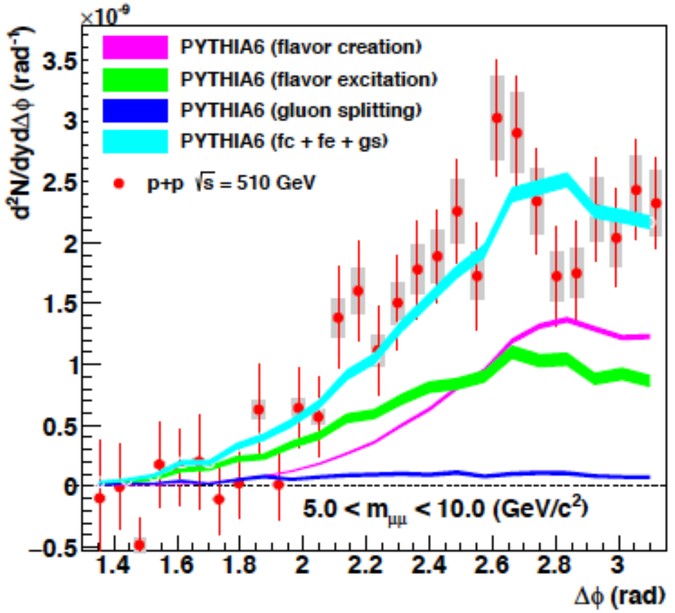

arXiv:2005.14276

Dominant at RHIC

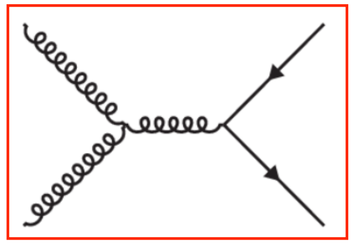

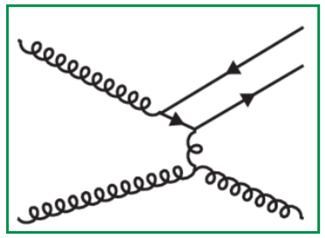

Dominant at LHC

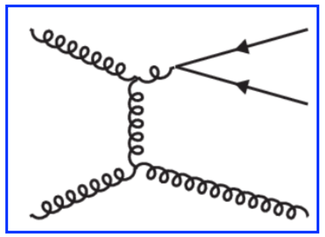

Heavy Flavor studies at PHENIX

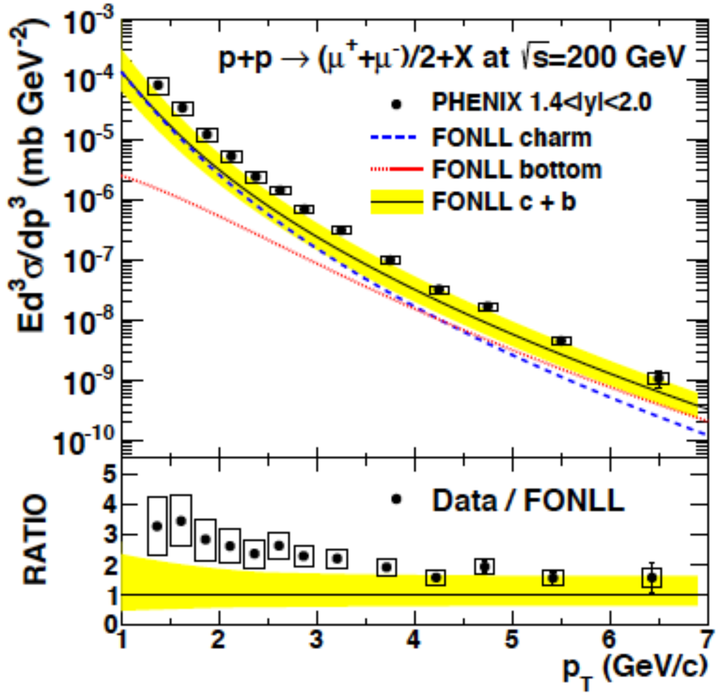

Invariant cross section of muons from open heavy-flavor decays in p+p collision at $\sqrt{s_{NN}} = 200$ GeV

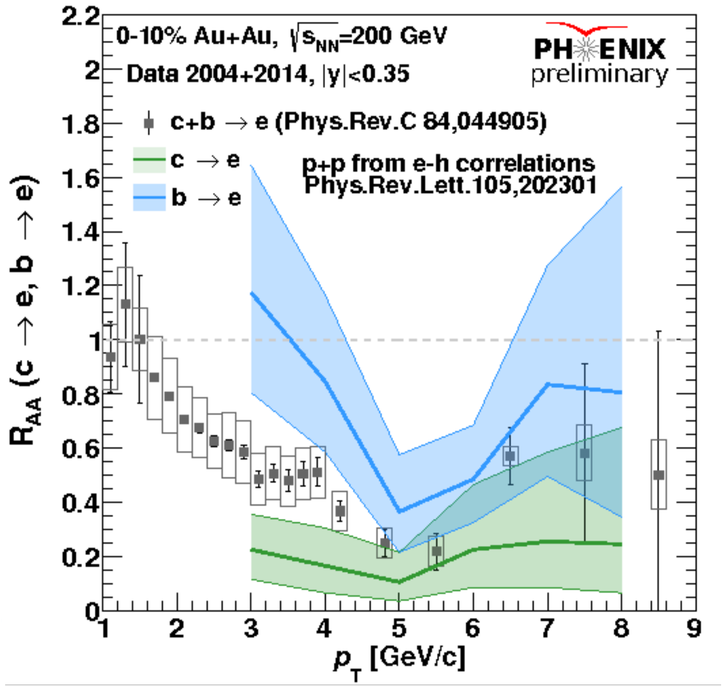

c/b separated R_{AA} using single electron data at $\sqrt{s_{NN}} = 200$ GeV

- Single muons from separated D and B hadrons have not yet been studied at forward rapidity at RHIC.
- PHENIX has a unique ability to carry out c/b separated heavy flavor study at low p_T and forward rapidity bins.
  - Can probe mass/flavor dependent energy loss mechanism in QGP.

PhysRevD.95.112001

Kinematics acceptance of heavy flavor decay products

- **MuTr**, **MuID** and **FVTX** make up the muon-arm.
- 1.2<|η|<2.2(2.4) for south(north) arm, full azimuthal coverage.
- ~10 int length absorbers to reject hadronic background.
- Hit in the VTX (|η|<1.0) constraints FVTX tracks in ϕ.

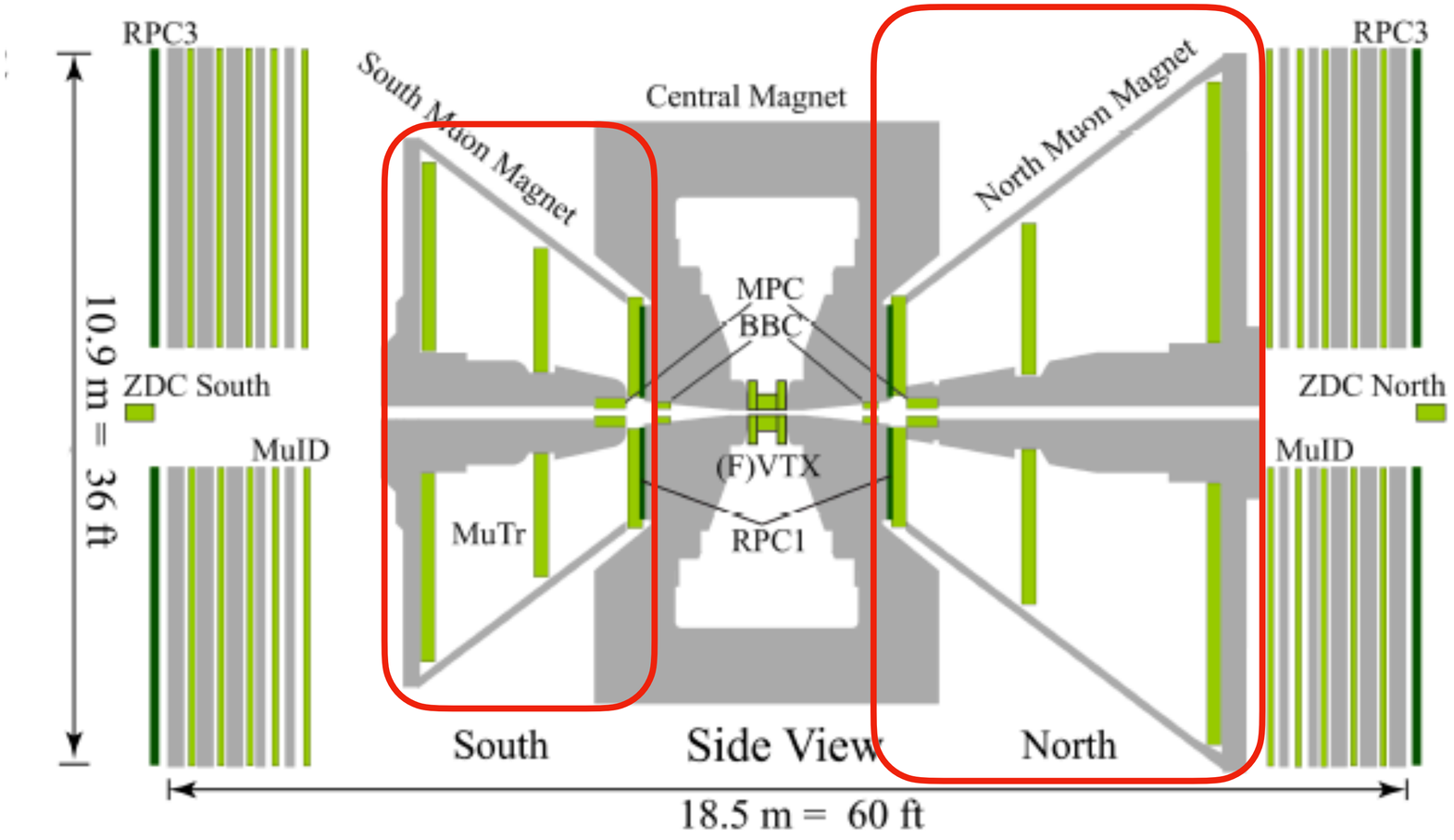

3 stations of cathode strip chambers for charged particle tracking

Kinematics acceptance of heavy flavor decay products

- **MuTr**, **MuID** and **FVTX** make up the muon-arm.
- 1.2<|η|<2.2(2.4) for south(north) arm, full azimuthal coverage.
- ~10 int length absorbers to reject hadronic background.
- Hit in the VTX (|η|<1.0) constraints FVTX tracks in ϕ.

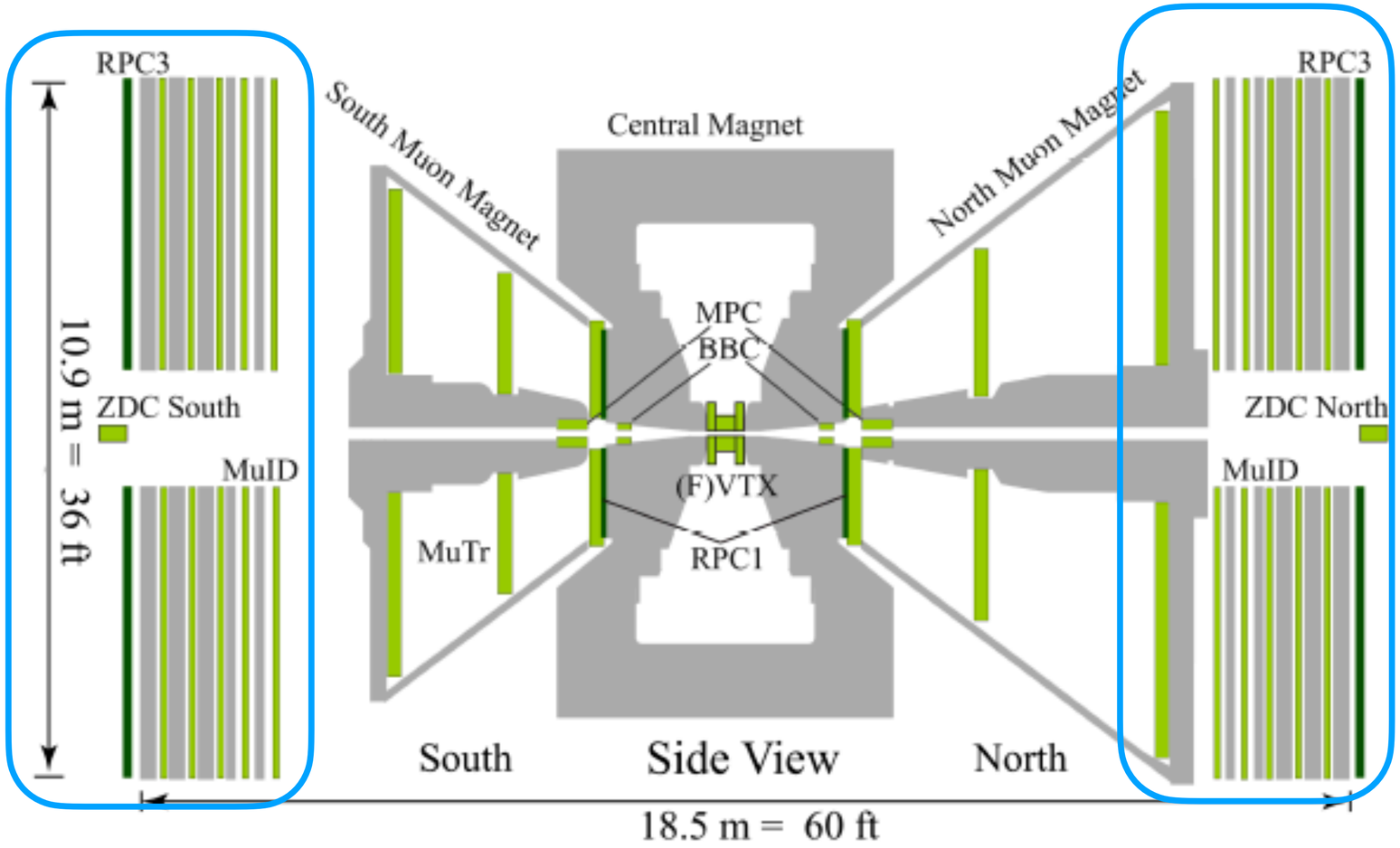

Alternating layers of plastic proportional tubes for muon identification and steel absorbers

Kinematics acceptance of heavy

- **MuTr**, **MuID** and **FVTX** make up the muon-arm.
- 1.2<|η|<2.2(2.4) for south(north) arm, full azimuthal coverage.
- ~10 int length absorbers to reject hadronic background.
- Hit in the VTX (|η|<1.0) constraints FVTX tracks in ϕ.

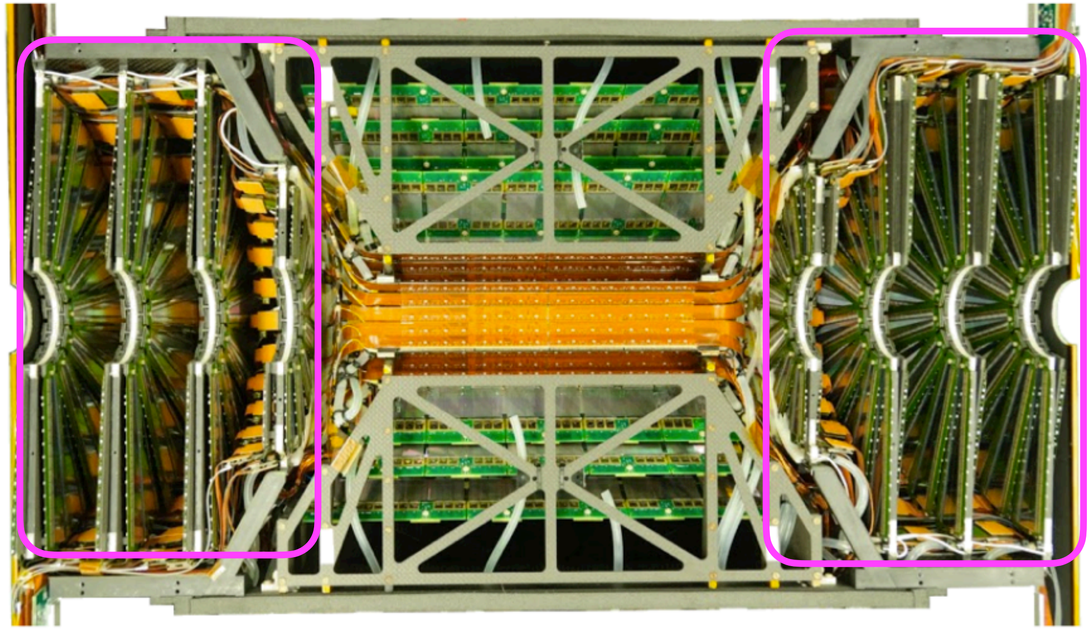

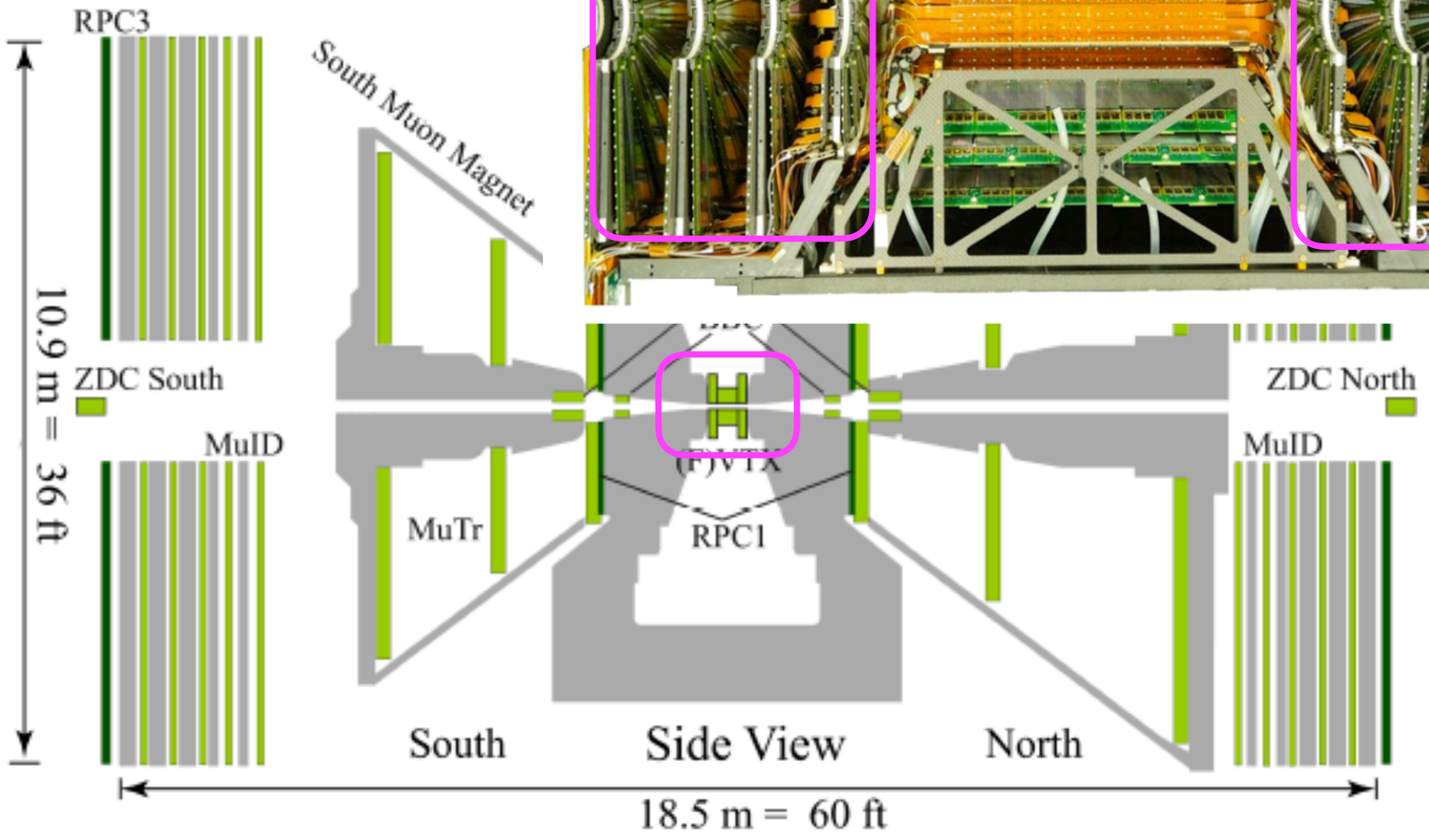

Vertex detectors for precise tracking and vertex measurement

Model comparison

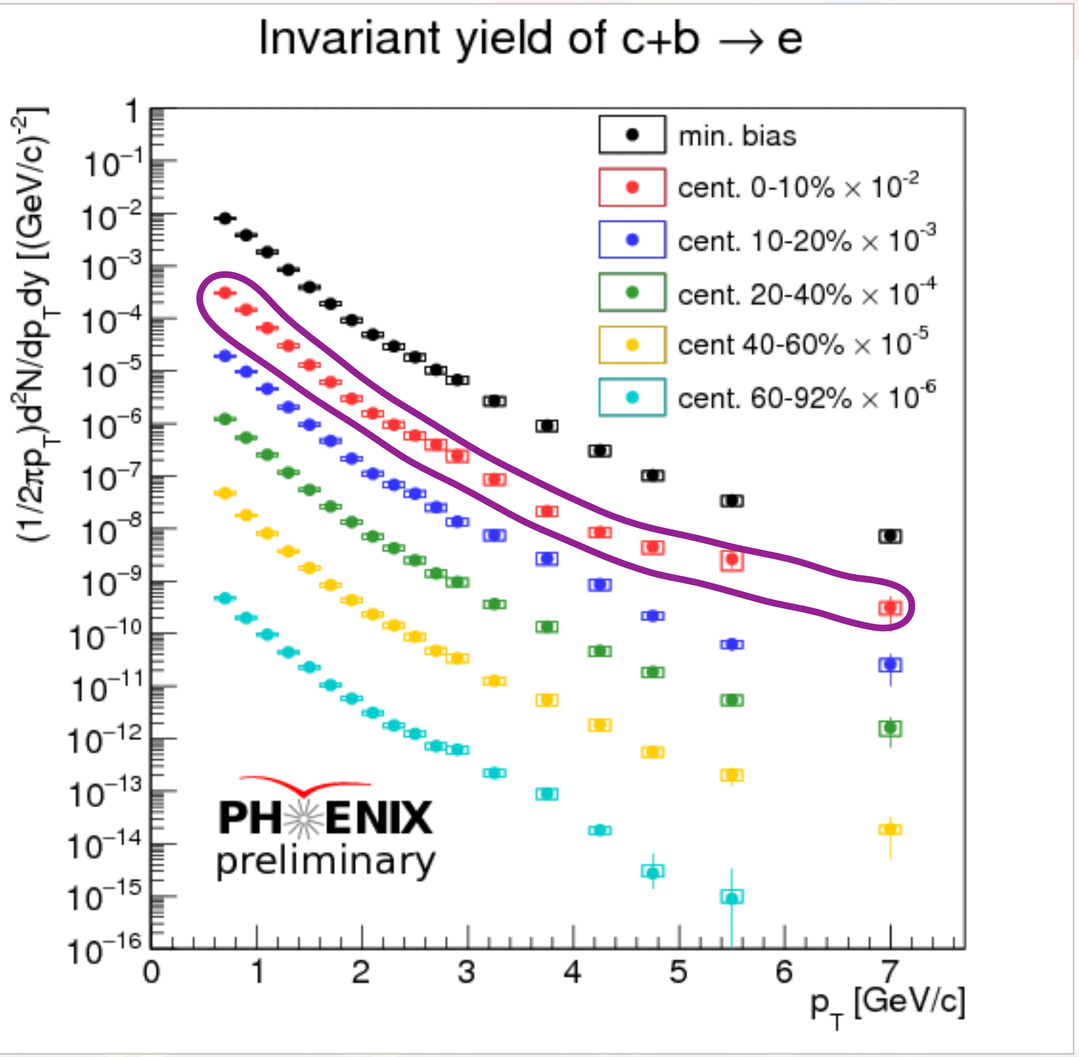

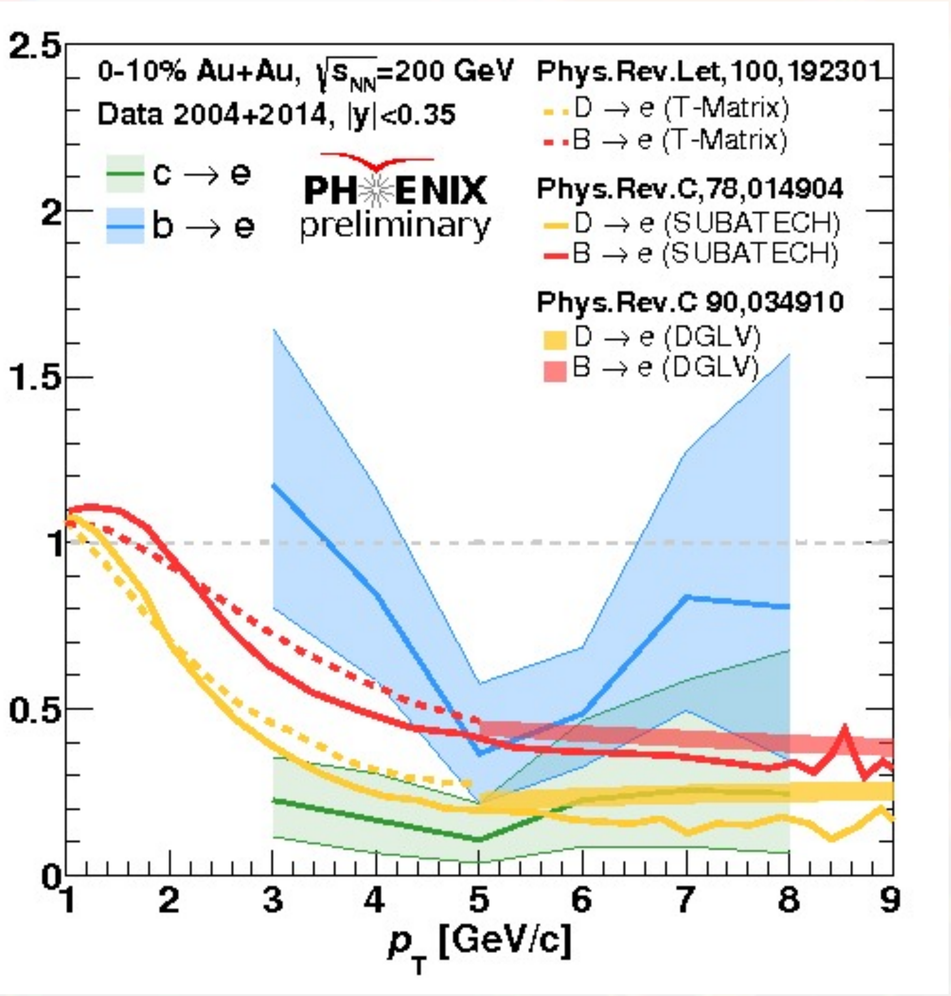

- T-Matrix: (T-Matrix + small diffusion const ($2\pi TD = 4$). Strong QGP coupling.
- SUBATECH: Boltzmann equation + running coupling + realistic hard thermal loop calculations.
- DGLV: Energy loss + plasma w/ static potentials.
- More precise measurement needed to distinguish between different models.

b-fraction model comparison

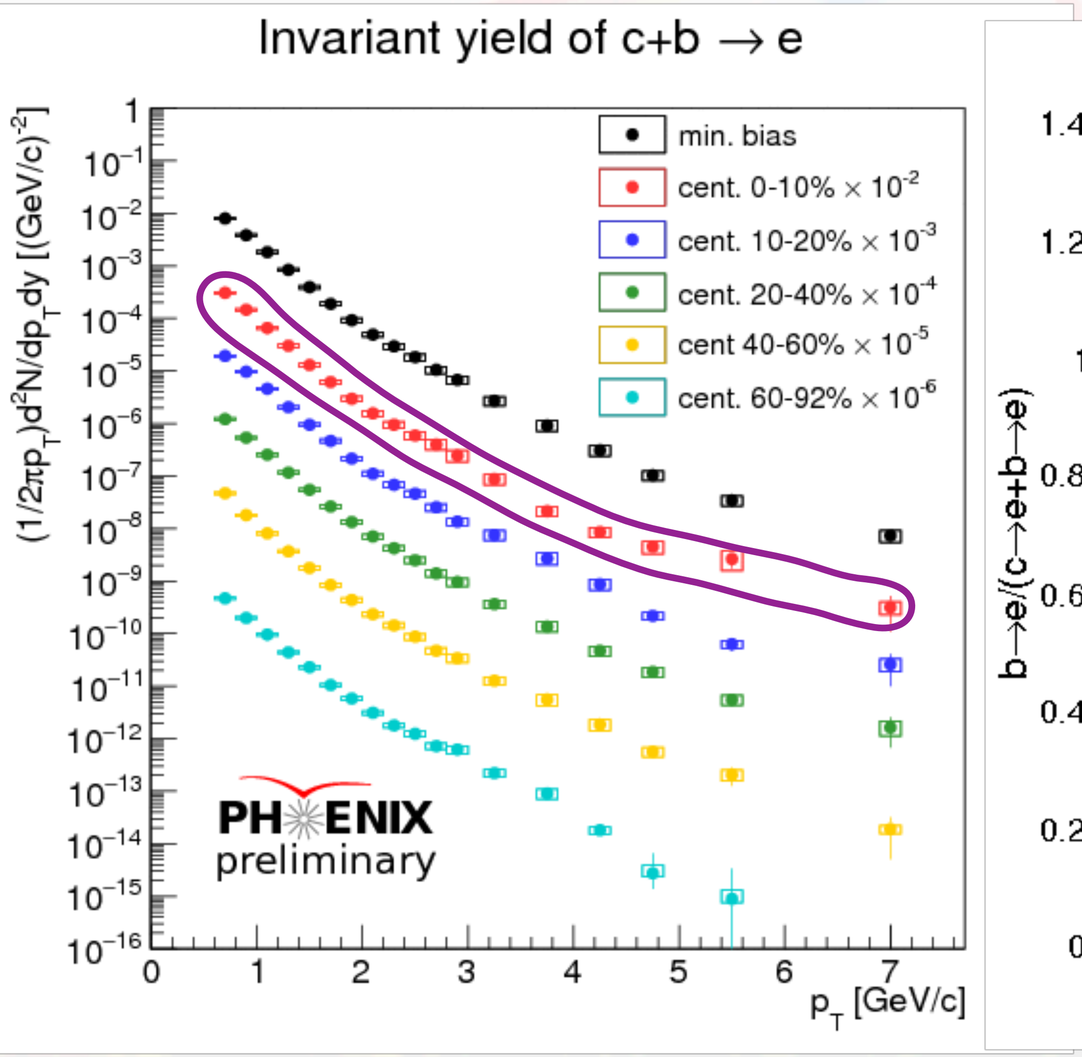

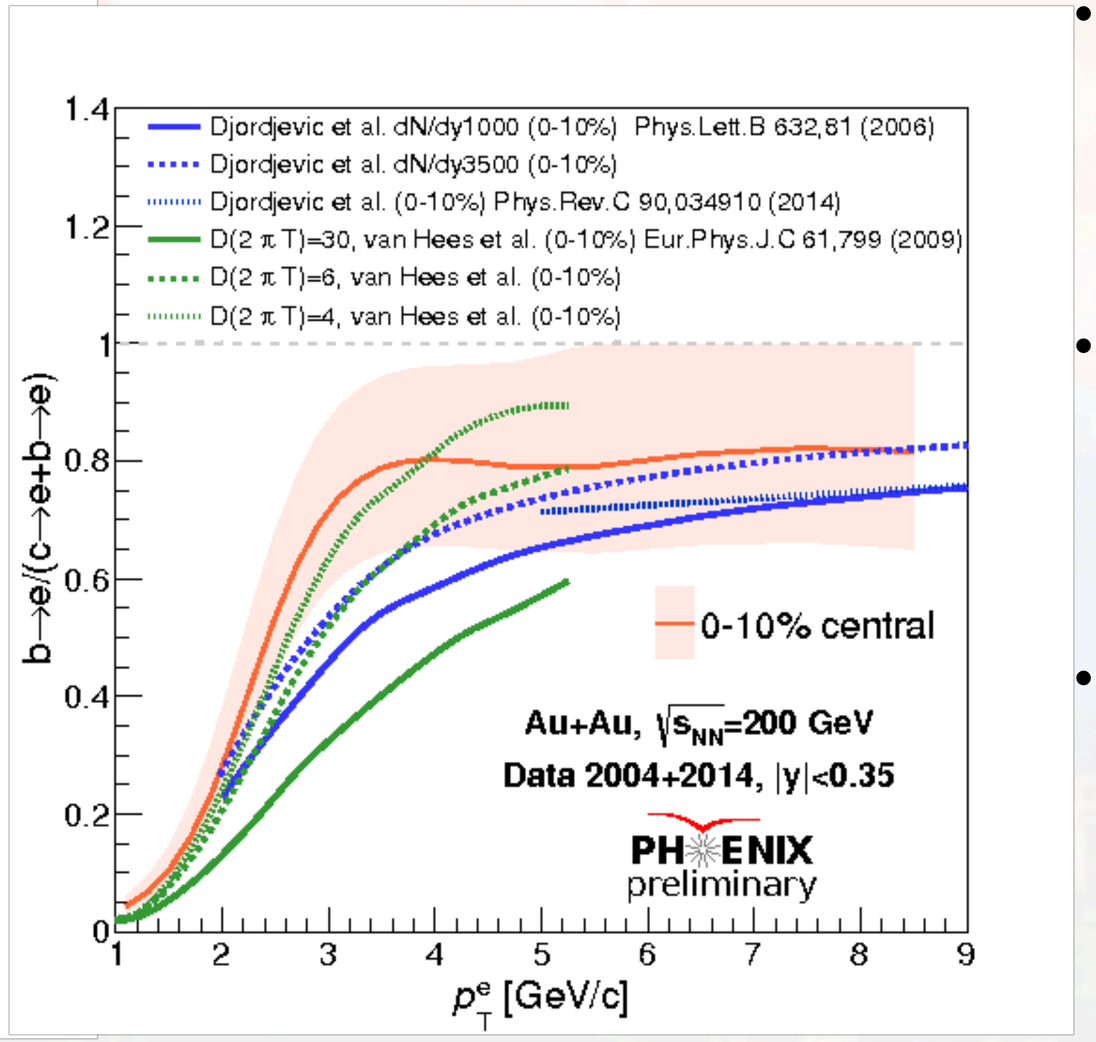

- T-Matrix + small diffusion const ($2\pi TD = 4/6$): Consistent with data.
- T-Matrix + large diffusion const ($2\pi TD = 30$) inconsistent with data.
- DGLV models: More precise measurement needed to separate between DGLV models with different gluon densities.